# EVALUATION OF CFTR INHIBITORY ACTIVITY OF MANGOSTEEN EXTRACTS AND HYDROXYXANTHONE DERIVATIVES

A THESIS

BY

WATINEE KUMPUM

Presented in Partial Fulfillment of the Requirements for the

Master of Science Degree in Chemistry

at Srinakharinwirot University

May 2014

# EVALUATION OF CFTR INHIBITORY ACTIVITY OF MANGOSTEEN EXTRACTS AND HYDROXYXANTHONE DERIVATIVES

A THESIS

BY

WATINEE KUMPUM

Presented in Partial Fulfillment of the Requirements for the

Master of Science Degree in Chemistry

at Srinakharinwirot University

May 2014

# EVALUATION OF CFTR INHIBITORY ACTIVITY OF MANGOSTEEN EXTRACTS AND HYDROXYXANTHONE DERIVATIVES

AN ABSTRACT

BY

WATINEE KUMPUM

Presented in Partial Fulfillment of the Requirements for the

Master of Science Degree in Chemistry

at Srinakharinwirot University

May 2014

Watinee Kumpum. (2014). *Evaluation of CFTR inhibitory activity of mangosteen extracts and hydroxyxanthone derivatives.* Dissertation, M.Sc. (Chemistry). Bangkok: Graduate School, Srinakharinwirot University. Advisor Committee: Assoc. Prof. Dr. Sunit Suksamrarn, Asst. Prof. Dr. Siritron Samosorn.

Secretory diarrhea is an important heath problem. This disease is commonly caused by intestinal infection with *Vibrio cholera*. *V. cholera* produces the cholera toxin to intracellular cAMP in intestinal epithelial cells and activates $Cl^-$ secretion of CFTR protein, is the main course for dehydration. Thus, the inhibition $Cl^-$ secretion of CFTR protein is a one for treatment secretory diarrhea. A series of hydroxyxanthen-9-one derivatives (**30-36**) were synthesized in 2-71 % yields from an oxidative coupling reaction between the corresponding *o*-hydroxybenzoic acids and activated phenols. All synthesized compounds were evaluated as potential inhibitors of CFTR by short circuit current analysis. The result showed that 1,3,6-trihydroxyxanthone (**34**) was the most potent CFTR inhibitor with 52 % inhibition at 100 $\mu$M and an $IC_{50}$ value of ~100 $\mu$M. This is the first report on hydroxyxanthones act as CFTR inhibitor which might be prospect for future development of pharmacotherapy for cholera.

In Thai folk medicine, the dried fruit pericarp of *G. mangostana* has been long used for treating diarrhea. However, the effect of mangosteen pericarp extract on $Cl^-$ secretion has never been investigated. The present study was therefore conducted to investigate the effect of the mangosteen extract on cAMP-activated $Cl^-$ secretion. Thus five mangosteen pericarp extracts (**E1-E4** and **E-7**) were prepared and evaluated for CFTR inhibitory activity on T84 cell and FRT cells by short circuit current analysis. The results showed that at concentration 50 $\mu$g/ ml only the 60% ethanol-water extract (**E4**) inhibited on db-cAMP-induced $Cl^-$ secretion by 60 %, where as other extracts were inactive under the same screening. Following fractionating of the active extract with $CH_2Cl_2$-water system, unfortunately, the resulting $CH_2Cl_2$ and aqueous fractions (**E-5** and **E-6**) were also inactive on the same test.

.

# การศึกษาฤทธิ์ในการยับยั้งการทำงานของโปรตีน CFTR ของสารสกัดมังคุด และอนุพันธ์ของไฮดรอกซีแซนโทน

บทคัดย่อ

ของ

วาทินี คุ้มพุ่ม

เสนอต่อบัณฑิตวิทยาลัย มหาวิทยาลัยศรีนครินทรวิโรฒ เพื่อเป็นส่วนหนึ่งของการศึกษา

ตามหลักสูตรวิทยาศาสตรมหาบัณฑิต สาขาวิชาเคมี

พฤษภาคม 2557

วาทินี คุ้มพุ่ม. (2014). *การศึกษาฤทธิ์ในการยับยั้งการทำงานของโปรตีน CFTR ของสารสกัดมังคุดและอนุพันธ์ของไฮดรอกซีแซนโทน*. ปริญญานิพนธ์ วท.ม. (เคมี). กรุงเทพฯ: บัณฑิตวิทยาลัย มหาวิทยาลัยศรีนครินทรวิโรฒ. อาจารย์ที่ปรึกษาปริญญานิพนธ์: รองศาสตราจารย์ ดร.สุนิตย์ สุขสำราญ, ผู้ช่วยศาสตราจารย์ ดร.สิริธร สโมสร.

โรคอหิวาตกโรคเป็นปัญหาสุขภาพที่สำคัญ ที่มีสาเหตุมาจากการติดเชื้อแบคทีเรีย *Vibrio cholera* ที่บริเวณลำไส้เล็ก เชื้อ *V. cholera* จะปล่อยสารพิษ cholera toxin เข้าสู่ภายในเซลล์ ส่งผลทำให้ cAMP ในลำไส้เล็กเพิ่มมากขึ้น กระตุ้นการขับคลอไรด์ไอออนของโปรตีน CFTR เพิ่มมากขึ้น ซึ่งเป็นสาเหตุหลักของการสูญเสียน้ำของร่างกาย ดังนั้นการยับยั้งการขับคลอไรด์ไอออนของโปรตีน CFTR เป็นทางเลือกหนึ่งในการรักษาโรคอหิวาตกโรค จากการศึกษาเบื้องต้นอนุพันธ์ของไฮดรอกซีแซนโทน (**30-36**) และสารสกัดจากมังคุด (**E1-E9**) ได้ถูกนำมาทดสอบฤทธิ์ในการยับยั้งขับคลอไรด์ไอออนของโปรตีน CFTR ของ T84 เซลล์ และ FRT เซลล์ ด้วยเทคนิค short circuit current analysis โดยพบว่า 1,3,6-trihydroxyxanthone (**34**) มีฤทธิ์ที่ดีที่สุดในการยับยั้ง CFTR ที่ 52 % ที่ความเข้มข้น 100 $\mu$M และ $IC_{50}$ ~100 $\mu$M นอกจากนี้สารสกัดมังคุดชั้น 60 % EtOH-$H_2O$ (**E4**) มีฤทธิ์ในการยับยั้งการขับคลอไรด์ไอออนโปรตีน CFTR ได้ 60 % ณ ความเข้มข้น 50 $\mu$g/ ml และจากการนำสารสกัดชั้น 60 % EtOH-water มาทำการสกัดด้วย $CH_2Cl_2$-water โดยผลจากการทดสอบพบว่า สารสกัดชั้น $CH_2Cl_2$ (**E5**) และ สารสกัดชั้นน้ำ (**E6**) ไม่มีฤทธิ์ในการยับยั้งการขับคลอไรด์ไอออนของโปรตีน CFTR

.

The thesis titled

"Evaluation of CFTR inhibitory activity of mangosteen extracts
and hydroxyxanthone derivatives"

By

Watinee Kumpum

has been approved by the Graduate School as partial fulfillment of the requirements for the Master of Science Degree in Chemistry of Srinakharinwirot University.

.

..... Dean of Graduate School
(Assoc. Prof. Dr. Somchai Santiwatanakul)
May , 2014

Dissertation Committee

..... Major-advisor
(Assoc. Prof. Dr. Sunit Suksamrarn)

..... Co-advisor
(Asst. Prof. Dr. Siritron Samosorn)

Oral Defense Committee

..... Chair
(Assoc.Prof. Dr. Thanuttkhul Mongkolaussavarat)

..... Committee
(Assoc. Prof. Dr. Sunit Suksamrarn)

..... Committee
(Asst. Prof. Dr. Siritron Samosorn)

..... Committee
(Asst. Prof. Dr. Mayuso Kuno)

# Acknowledgements

I would like to take this opportunity to express my sincere gratitude to the people who are in one way or another played a role in making this dissertation possible.

First and foremost, I would like to thank my research advisor Assoc. Prof. Dr. Sunit Suksamrarn for her deeply and constantly generosity, valuable guidance and encouragement throughout this study. I also would like to acknowledge my co-advisor, Asst. Prof. Dr. Siritron Samosorn for her valuable guidance and suggestions.

I would like to thank all my thesis committee members, Assoc.Prof. Dr Thanuttkhul Mongkolaussavarat, Chulabhorn Graduate Institute and Asst. Prof. Dr. Mayuso Kuno for their endless kindness, thoughtful advice, valuable time, patient reading and warm encouragement.

I am grateful to supports from the Center of Excellence for Innovation in Chemistry (PERCH-CIC) and The Thailand Research Fund.

I would like to thank Assist. Prof. Dr. Chatchai Muanprasat, Department of Physiology, Faculty of Science, Mahidol University for bioactivity evaluation and to Assist. Prof. Dr. Boon-ek Yingyongnarongkul, Department of Chemistry, Faculty of Science, Ramkhamhaeng University for recording mass spectra.

I am grateful to my seniors, Mr. Thongchai Khammee and Ms. Amornmart Jaratrungtawee for their assistance in the laboratory. I appreciate their guidance, invaluable help and also our friendship as well, this made research full with enjoyable experience. I would like to thank Ms. Natthakaln Lomchoey, for recording the nuclear magnetic resonance spectra.

A special acknowledgement extends to department of chemistry, faculty of science, Srinakharinwirot university for providing research facilities, including all of people whom my thesis are concerned with. Their assistance can greatly encourage and improve my work all the time it proceeded.

Finally, I wish to express my profound gratitude to my parents and family for their love, unconditional support and encouragement throughout my whole life.

Watinee Kumpum

# TABLE OF CONTENTS

TABLE OF CONTENTS (continued)

# LIST OF FIGURES

# LIST OF TABLES

# CHAPTER 1
# INTRODUCTION

Secretory diarrhea is an important heath problem. In developing countries, secretory diarrhea is the second leading cause of death in children under five years. This disease is commonly caused in intestinal infection by gram-negative bacillus, *Vibrio cholera*, which is transmitted through contaminated food and water when is untreated, leads to severe dehydration and shock. *V. cholera* produces the cholera toxin to intracellular cAMP in intestinal epithelial cells and activates $Cl^-$ secretion, is the major driving force for fluid secretion (Thiagarajah and Verkman 2005; 172-174).

## 1. Secretory diarrhea medications

Currently, there are several anti-diarrhea drugs on the markets but they are ineffective to treat diarrhea. Diarrhea therapy with oral rehydration solutions (ORS) is the main to increase the minerals but it is unable to prevent the dehydration. The new researching approaches for treating diarrhea are as follow. (Thiagarajah and Verkman 2005; 172-174)

### 1.1 Cholera vaccines and antibiotics

Cholera vaccines have been used in cholera treatment for more than 100 years. Cholera vaccines have been shown in endemic areas such as Peru, Bangladesh and Micronesia which particularly against the *V. cholera* EI Tor biotype. However, they have shown short biological half-life for agonistic the *V. Cholera* and low efficacy in under 5-year children. In addition, antibiotic drugs such as tetracycline and furazolidone were used to reduce the severity of only diarrhea because it has the short length of protection.

### 1.2 Inhibition of cholera toxin (CT) – receptor binding

Another approach to reduce diarrhea in cholera is the inhibition of CT binding on intestinal enterocytes. Cholera toxin, *Vibrio cholera*, binds to GM1 ganglioside receptor,

retrograde endocytosis to epithelial cell and activation of adenylate cyclase (AC). Resulting, intracellular cAMP increases, which stimulates salt and fluid secretion on the cystic fibrosis transmembrane conductance (CFTR) $Cl^-$ channel. So, the inhibition of cholera toxin binding is an important target for treating diarrhea.

### 1.3 Enkephalinase inhibitors

The enkephalins are rapaidly degraded by a dipeptidyl carboxylase known as enkephalinase. They are endogenous opiate substances that prevent fluid secretion by binding to delta opioid peptide receptors in enterocytes. After that, enkephalins will stimulate G proteins (Gi) for inhibitory CFTR $Cl^-$ channel and basolateral $K^+$ channel, resulting can be reduced secretion of salt and fluid. In clinical, racecadotril as enkephalinase inhibitor, was effective against *V. cholera* and *E. coli* in pediatrics diarrhea. But it is not effective for adult because absorption in the intestine is rapidly.

### 1.4 CFTR inhibitors

Another potential target for anti-secretory therapy is the CFTR inhibitor. CFTR is a protein that controls fluid, $Cl^-$ ions of epithelial cell and other enterotoxin-mediated secretory diarrheas. CFTR Inhibitors such as thiazolidone (CFTRinh-172), glycine hydrazine (GlyH-101) which were discovered by high-throughput screening, have been shown effective inhibitors to inhibit $Cl^-$ ion and fluid secretion in human intestinal cells. Up to date 8 types of compounds are reported as CFTR inhibitors. These are arylaminobenzoic acid, sulfonylureas, thiazolidinone, glycine hydrazine, flavanoids, tannin, quinazolin and proanthocyanidin. The search for new pharmacophores for CFTR inhibitory activity, however, remains to be important.

*G. mangostana* or mangosteen is a rich source of natural polyphenol compounds such as tannins, flavonoids and xanthones. *G. mangostana* pericarp has been used as traditional medicine for treating diarrhea and dysentery, however, its CFTR inhibitory activity has not been studied. Our interest in the bioactive compounds of *G. mangostana* along with the long history usage of mangosteen pericarp as anti-diarrhea agent prompt us to explore the

active substance and/ or fractionate of the pericarp as CFTR inhibitors. In addition, in a preliminary screening showed that the major prenylated xanthone, $\alpha$-mangostin, from *G. mangostana* was a very weak inhibitor for blocking $Cl^-$ of CFTR channel. It is therefore of interest to identify other xanthones that would be more potent CFTR inhibitor than that of *G. mangostana* xanthone. Considering functional groups in $\alpha$-mangostin, an oxygenated xanthone comprising two prenyl groups in its scaffold, the prenyl moieties should play an important role for such low activity. Therefore, hydroxyxanthones without prenyl group is designed and synthesized, followed by evaluations for their CFTR inhibitory activity.

## Objectives of the study

1. To identify the active substance and/or fractionates obtained from *G. mangostana* pericarp as CFTR inhibitor.

2. To synthesize and evaluate hydroxyxanthone derivatives as CFTR inhibitors.

# CHAPTER 2
# REVIEW OF LITERATURES

## 1. The cystic fibrosis transmembrane conductance regulator (CFTR)

CFTR is a chloride channel in the apical membrane of epithelial cells, including lung, liver, pancreas, digestive tract, reproductive tract, and skin. CFTR is regulated by cAMP-dependent protein kinase (PKA) and ATP. This includes two transmembrane domains (TMDs), two intracellular nucleotide-binding domains (NBD1 and NBD2) and one unique intracellular regulatory (R) domain. The NBD1 and NBD2 connect with two adenosine triphosphate (ATP) at LSHGH and LSGQQ sequence, respectively and R domain connect with NBD1 to TMD2 (Figure 1). (Zhang et al. 2012; 329-345)

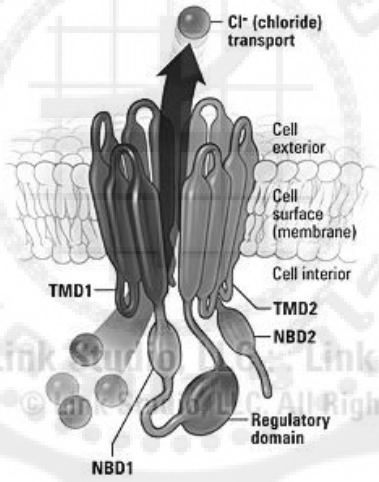


Figure 1 Structure of the cystic fibrosis transmembrane conductance regulator (CFTR) (Link studio. (2014). Cystic fibrosis transmembrane conductance regulator http. Retrived 2 3, 2014, from http://www.linkstudio.info/portfolio/illustration05.htm.)

### 1.1 Process of channel opening and closing

CFTR is an ABC transporter, meaning that it uses ATP to open and close channel. Phosphorylation of the R domain allows for the first ATP molecule to bind the NBD1 at LSHGH sequence and the second ATP molecule attract at LSGQQ sequence of NBD2, and a signal is

transmitted to allow for the opening of the channel. After that, the ATP molecules of NBD2 is hydrolyzed to ADP (thereby releasing a phosphate group), the channel begins to close (Figure 2). (Zhang et al. 2012; 329-345)

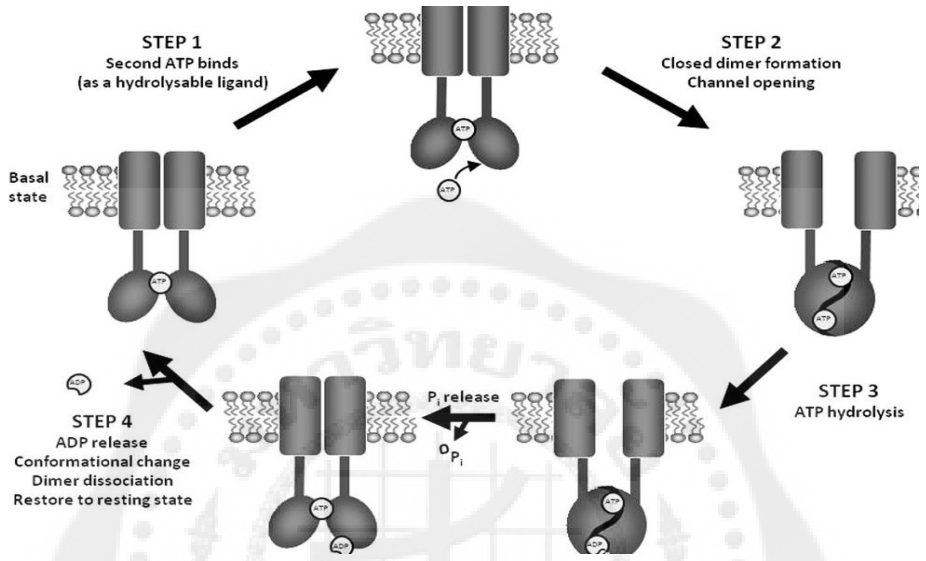


Figure 2 Process of ATP binding, channel opening and closing (Gout. 2012; 115-121)

### 1.2 Inhibition of the CFTR $Cl^-$ channel

There are two pathways of inhibition on the CFTR $Cl^-$ channel

#### 1.2.1 Open channel blockers

Inhibition CFTR $Cl^-$ channel by large anion ($A^-$) on the activity of the CFTR $Cl^-$ channel. Large anions inhibit CFTR by occluding the intracellular end of the channel pore and $Cl^-$ prevention (Figure 3). (Zhiwei et al. 2004; 141-147)

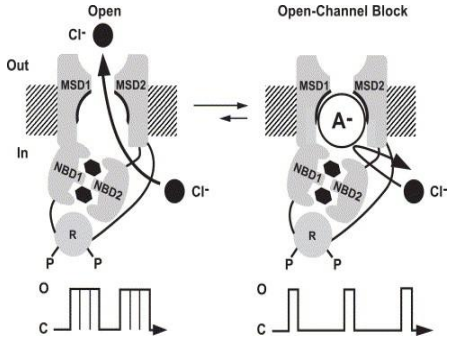


Figure 3 Inhibition of the CFTR $Cl^-$ channel by open channel blockers (Zhiwei et al. 2004; 141-147)

1.2.2 Allosteric blockers

Allosteric blockers, genistein, inhibit CFTR by greatly slowing the rate of channel opening. As a result, in the presence of these agents, the duration of closed periods separating channel openings is greatly prolonged.

Genistein blocks CFTR by an allosteric mechanism. This simplified model shows the effect of elevated genistein (G) concentrations on the activity of the CFTR $Cl^-$ channel (Figure 5). Elevated genistein concentrations inhibit CFTR principally by slowing greatly the rate of channel opening. Because elevated concentrations of ATP relieve genistein inhibition of CFTR, we propose that genistein and ATP compete for a common binding site (Figure 4). (Zhiwei et al. 2004; 141-147)

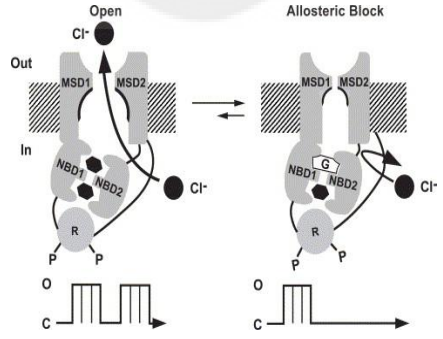


Figure 4 Inhibition of the CFTR $Cl^-$ channel by allosteric blocker (Zhiwei et al. 2004; 141-147)

### 1.3 Targeting CFTR for therapy of secretory diarrhea

#### 1.3.1 CFTR activators

CFTR activation requires elevation of intracellular cAMP and the consequent phosphorylation at the R domain by protein kinase A (PKA). ATP binding and possibly hydrolysis at NBDs are also required for channel opening. Negative regulatory mechanisms involve degradation of cAMP by phosphodiesterases (PDEs) and CFTR dephosphorylation by phosphatases (PPases). CFTR activators is direct inhibition on CFTR protein, or indirectly by inhibiting PDEs (thus elevating cAMP) or inhibiting PPases (thus increasing CFTR phosphorylation). Indirect effects are not expected to be useful for cystic fibrosis pharmacotherapy as the basic defect is intrinsic to the CFTR protein and not to upstream regulatory pathways (Figure 5). (Galietta et al. 2004; 497-503)

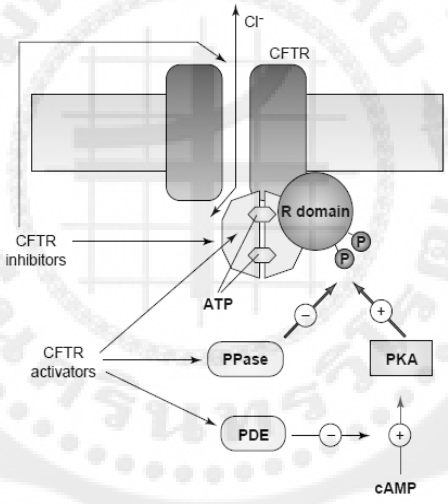


Figure 5 Pharmacological mechanisms for CFTR activation and inhibition (Galietta et al. 2004; 497-503)

CFTR activators by direct and indirect interaction include small molecules of, for examples, xanthine (such as IBMX (**1**)), benzimidazolones (such as NS004 (**2**)), benzo[c]quinoliziniums (such as UCCF-029 (**3**), CFTRact-09 (**4**), and CFTRact-12 (**5**)) and flavones/isoflavone (such as genistein (**6**)) (Figure 6). (Thiagarajah and Verkman 2003; 594–599)

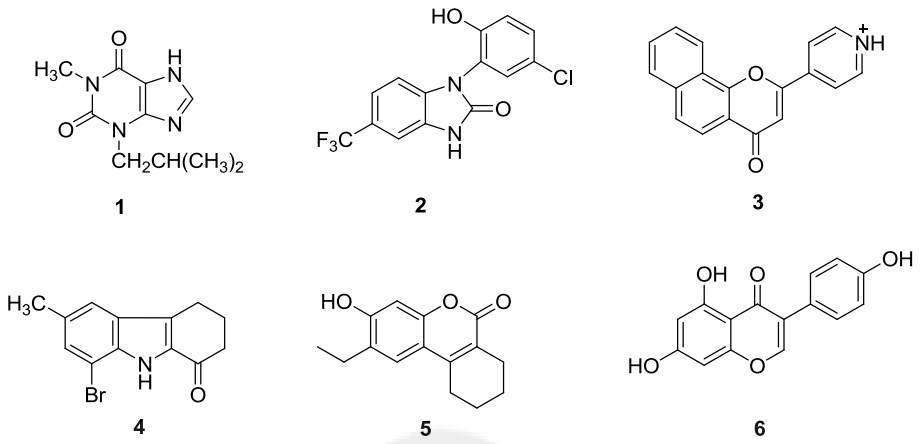


Figure 6 Chemical structures of CFTR activators of IBMX (**1**), NS004 (**2**), UCCF-029 (**3**), CFTRact-09 (**4**), CFTRact-12 (**5**) and genistein (**6**)

1.3.2 CFTR Inhibitors

Specific CFTR inhibitors could either block the channel pore or affect the gating mechanisms (Figure 5). Up to 2013, there have been reported 8 types of compounds as CFTR inhibitors, these are arylaminobenzoic acid, sulfonylureas, thiazolidinone, glycine hydrazine, flavanoids, tannin, quinazolin and proanthocyanidin.

1.3.2.1 Arylaminobenzoates

Hwang reviewed that diphenylamine-2-carboxylate or DPC (**7**) and 5-nitro-2-(3-phenylpropylamino)-benzoic acid or NPPB (**8**) (Figure 7) were discovered as CFTR inhibitors by screening over 200 compounds. Compounds **7** and **8** inhibited CFTR channel with haft-maximal inhibition ($K_i$) 526 $\mu$M and 580 nM, respectively. However, a different explanation was represented by Mccarty et al in 1993. They showed that DPC (**7**) induced inhibition of CFTR $Cl^-$ channel was voltage dependent and occluded the CFTR $Cl^-$ channel pore. (Hwang and Sheppard 1999; 448-453).

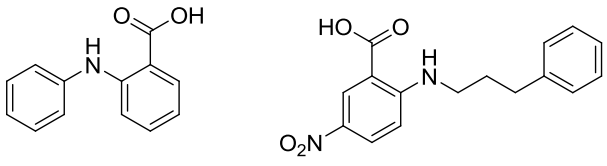

**7** **8**

Figure 7 Chemical structures of DPC (**7**) and NPPB (**8**)

1.3.2.2 Sulfonylureas

In 1999, Hwang et al. reviewed that sulfonylureas, glibenclamide (**9**) and tolbutamide (**10**) (Figure 8), were group of hypoglycemia drugs for treating non-insulin dependent diabetes mellitus. These compounds binded to the ABC protein SUR, where it modulates Kir6.2 $K^+$ channel activity and insulin release from pancreatic islet cells. Like CFTR, SUR1 was a member of the ABC transporter family in CFTR protein. The effect of glibenclamide (**9**) and tolbutamide (**10**) was investigated to inhibit cAMP-stimulated $Cl^-$ currents. At higher concentrations, these compounds were likely to block CFTR function by binding to the CFTR pore in its open state. Compounds **9** and **10** inhibited cAMP-stimulated $Cl^-$ currents in cells expressing recombinant CFTR with a haft-maximal inhibition ($K_i$) at 20 and 150 $\mu$M, respectively. Although glibenclamide (**9**) has been widely used to inhibit CFTR, it was not a specific inhibitor of the CFTR $Cl^-$ channel (Hwang and Sheppard 1999; 448-453).

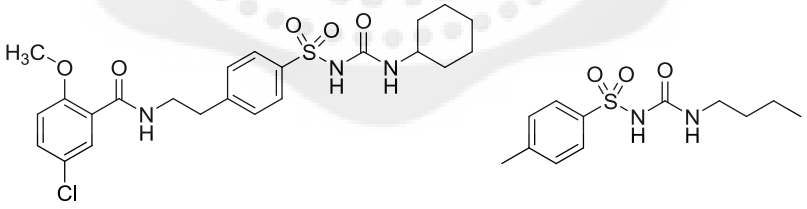

**9** **10**

Figure 8 Chemical structures of glibenclamide (**9**) and tolbutamide (**10**)

1.3.2.3 Thiazolidinone

In 2002, Ma et al. screened 50,000 compounds for inhibition of $Cl^-$ secretion in epithetail cells of CFTR, and found that 2-Thioxo-4-thiazolidone or CFTRinh-172 (**11**) was the most potent with half-maximal inhibition ($K_i$) 300 nM. Furthermore, CFTRinh-172 (**11**) was nontoxic at high concentrations and specific in cell culture and mouse models only. A single intraperitoneal injection of compound **11** (at the dose of 250 $\mu$g per kg of mice weight) in mice can reduce the cholera toxin-induced fluid secretion by more than 90% in the small intestine over 6 hours. Thiazolidinone CFTR inhibitors may be useful in developing large-animal models of cystic fibrosis and in reducing intestinal fluid loss in cholera and other secretory diarrheas (Ma et al. 2002; 1651-1658).

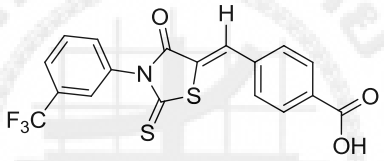


Figure 9 Chemical structure of CFTR inh-172 (**11**)

1.3.2.4 Glycine hydrazine

In 2004, Muanprasat et al. screened 100,000 small molecules for inhibition of CFTR $Cl^-$ channel and found that the group of glycine hydrazines was crucial for increasing inhibitory activity. Analysis of series of synthesized glycine hydrazine analogues exposed maximum inhibitory potency for *N*-(2-naphthalenyl) and 3,5-dibromo-2,4-dihydroxyphenyl substituents. The compound of *N*-2-(napthalenyl)-[(3,5-dibromo-2,4-dihydroxyphenyl)methylene]glycine hydrazine or GlyH-101 (**12**) (Figure 10) could inhibit CFTR $Cl^-$ conductance in <1 min. Furthermore, this compound inhibited CFTR Cl- conductance at >30 μM in whole-cell patch-pump and at 2.5 $\mu$g concentration reduced by ~80% cholera toxin–induced intestinal fluid secretion (Muanprasat et al. 2004; 125-137).

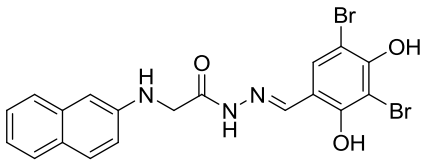


Figure 10 Chemical structure of GlyH-101 (**12**)

1.3.2.4 Flavanoids

In 2005, Schuier et al. studied the dose-dependent effects of flavonoid compounds from cocoa bean, including (+)-catechin (**13**), (-)-epicatechin (**14**), procyanidin B2 (**15**), quercetin (**16**), morin (**17**), lutiolin (**18**) and baicalein (**19**) (Figure 11). These compounds were tested on forskolin stimulated CFTR-mediated $Cl^-$ secretion across T84 colonic epithelia. It was found that (-)-epicatichin (**14**) was the most effective blocker with *Ki* in the range of 100 $\mu$M. Morin (**17**) and baicalein (**19**) were less effective blocker. These data indicated that cocoa flavanols targeted intestinal CFTR $Cl^-$ transport and may serve as inhibitors of cAMP-stimulated $Cl^-$ secretion in the intestine. (Schuier et al. 2005; 2320-2325)

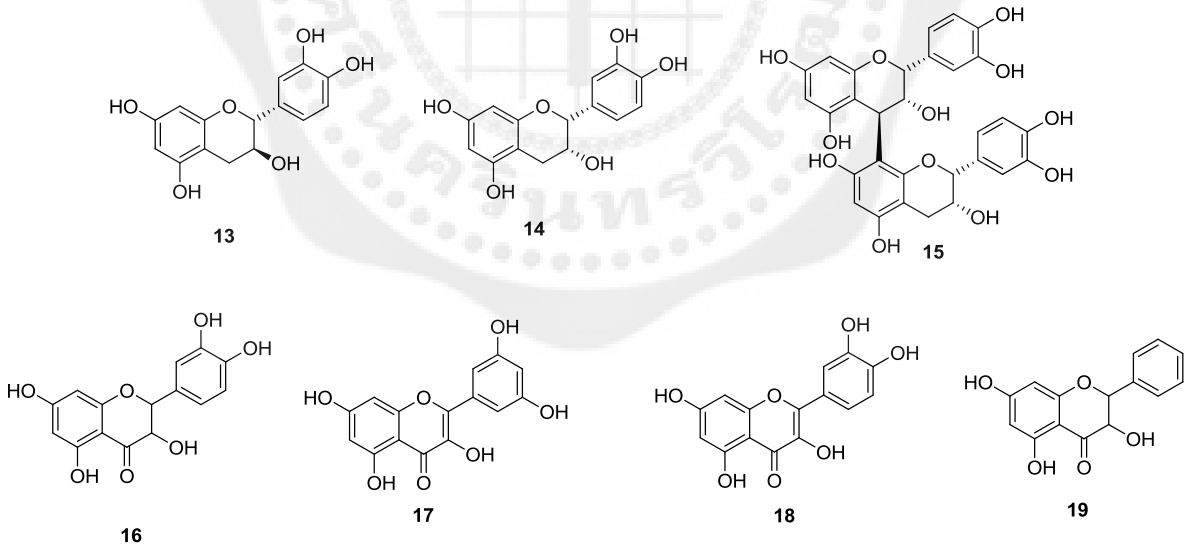


Figure 11 Chemical structures for (+)-catechin (**13**), (-)-epicatechin (**14**), procyanidin B2 (**15**), quercetin (**16**), morin (**17**), lutiolin (**18**) and baicalein (**19**)

1.3.2.5 Tannin

In 2010, Wongsamitkul et al. studied the effects and mechanisms of actions on CFTR protein of penta-*m*-digalloyl-glucose (PDG) or tannic acid (**20**) (Figure 12) obtained from the tannic extract of Chinese gallnut. This resulted that PDG (**20**) can inhibit on cAMP-activated chloride secretion in FRT cells and human intestinal cells (T84 cells) with $IC_{50} \cong 10\ \mu M$, without effects on intracellular cAMP content and cell viability. Furthermore, PDG (**20**) efficiently inhibited chloride secretion and no effect on calcium-induced chloride secretion in T84 cells. In mice, a single intraluminal injection of PDG (**20**) (0.6 mg/ kg) reduced cholera toxin-induced intestinal fluid secretion by 75% with no effect on intestinal fluid absorption (Wongsamitkul et al. 2010; 490-497).

In 2012, Ren et al. demonstrated that the tannic acid-based medical food, Cesinex®, was effective a good safety profile for treatment diarrhea at 0.01-0.1 mg/ml and inhibited the CFTR-dependent or the calcium-activated $Cl^-$ secretion (Ren et al. 2012; 99-108).

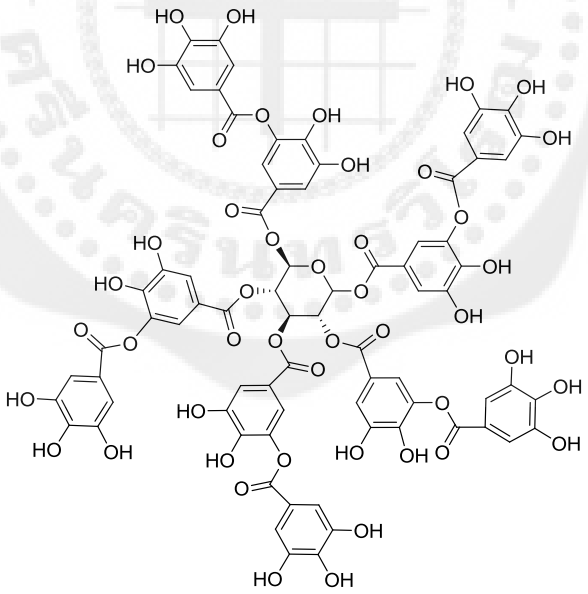

Figure 12 Chemical structure of PDG (**20**)

1.3.2.6 Quinazolin

In 2012, Patanatindee et al. studied the antidiarrheal efficacy and pharmacological of ethyl-2-(4-oxo-3-o-tolyl-3,4-dihydroquinazolin-2-ylthio)acetate, DQA, (**21**) (Figure 13) for using as a CFTR inhibitor in Fisher rat thyroid (FRT) cells expressing human CFTR and human intestinal epithelial T84 cells by short-circuit current measurements and MTT assays. In this result, DQA (**21**) inhibited chloride secretion with $IC_{50} \cong 20$ $\mu$M and complete inhibition at 200 $\mu$M. Furthermore, DQA (**21**) was nontoxic to FRT cells (5-500 $\mu$M) and effectively inhibited both forkolin and cholera toxin-induced transepithelial chloride secretion in T84 cells. In mice, DQA (**21**) at 100 $\mu$M reduced cholera toxin (1 $\mu$g/ closed loop)-induced intestinal fluid secretion by 85 % without affecting intestinal fluid absorption (Patanayindee et al. 2012; 619-613).

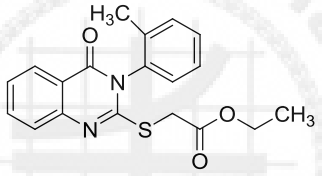


Figure 13 Chemical structure of DQA (**21**)

1.3.2.7 Proanthocyanidin

In 2012, Verkman et al. investigated the antisecretory diarrheal mechanism on calcium-activated chloride channels (CaCC) and CFTR $Cl^-$ channel of crofelemer (**22-28**) (Figure 14) obtained from the bark latex of *Croton lechleri*. Crofelemer (**22-28**) was an amorphous, dark red-brown powder consisting of an oligomeric proanthocyanidin of varying chain lengths with an average molecular weight of 2100 daltons. In this result, crofelemer (**22-28**) inhibited CFTR $Cl^-$ channel with maximum inhibition ~60% and $IC_{50}$ value of ~7 $\mu$M. A comparison study on the possible possibility site of action on CFTR between crofelemer and CFTR inhibitors, thiazolidinone (**11**) and glycine hydrazide (**12**), showed that crofelemer (**22-28**) inhibited at a outside of the CFTR pore because the larger size of **22-28** than thiazolidinone (11) and glycine hydrazide (**12**). Furthermore, crofelemer (**22-28**) were shown to strongly inhibit the intestinal

CaCC $Cl^-$ channel in TMEM16A protein with maximum inhibition >90% and $IC_{50}$ ~6.5 $\mu$M by a voltage-independent inhibition (Verkman et al. 2012; US 2012/0202876).

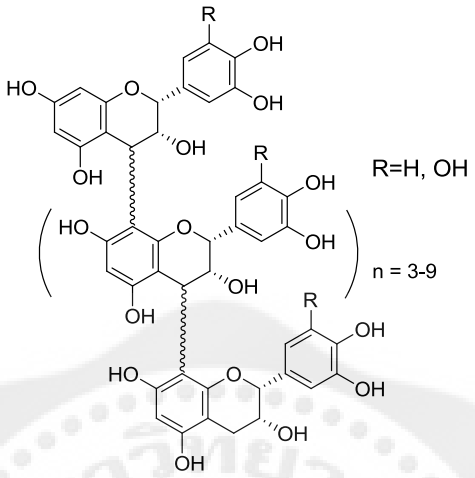


Figure 14 Chemical structures of crofelemer (22-28) from *C. lechleri*

# CHAPTER 3
# EXPERIMENTAL

## 1. Materials and methods

### 1.1 Solvents and chemicals

Chemicals reagents were obtained from Sigma Chemical Co., Aldrich Chemical Co., Fluka Chemie AG, and Acros Chemical Co and were used without further purification. The commercial grade solvents used for flash chromatography were distilled before use. Anhydrous solvents were stored over molecular sieves (4 Å).

### 1.2 Physical constants

All melting points were determined in glass capillaries using a Griffin melting point apparatus and are uncorrected.

### 1.3 Spectroscopic techniques

1.3.1 Nuclear magnetic resonance spectrometry (NMR)

The $^{1}$H-NMR and $^{13}$C-NMR (75 MHz) spectra and 2D-NMR Spectra were recorded on Bruker Avance 300 FT-NMR spectrometer. Samples were run either in deuteriochloroform ($CDCl_3$), deuteriomethanol ($CD_3OD$) or dimethylsulfoxide-$d_6$ (DMSO-$d_6$). The chemical shifts ($\delta$) were in ppm. The coupling constants were measured in Hz and the following abbreviations are adopted: s (singlet); d (doublet); t (triplet); q (quartet); m (multiplet); dd (doublet of doublets); dt (doublet of triplets). The complete assignment of all proton and carbon signals was completed via 1D proton and carbon NMR experiments.

1.3.2 Infrared spectrometry (IR)

Infrared (IR) spectra were taken as KBr pellets and/or as a solution in dichloromethane on a Perkin Elmer FT-IR spectrum BX.

1.3.2 Mass spectrometry

Electrospray ionization (ESI) mass spectra were obtained with a Finnigan LC-Q mass spectrometer (Department of chemistry, Faculty of Science, Rhamkhamhaeng University). Electrospray ionization-time-of-flight (ESI-TOF-MS) mass spectra (Bruker Daltonics GmbH, Bremen, Germany) were recorded with micrOTOF-Q II, an orthogonal acceleration quadrupole time-of-flight (Q-TOF) mass spectrometer equipped with electrospray interface (Archemica International Co, Ltd.).

**1.4 Chromatography**

Flash column chromatographic separations were carried out using silica gel (E. Merck, type 60, 230-400 mesh), precoated silica gel $GF_{254}$ preparative TLC plates (20 x 20, 0.5 mm thick, E. Merck). Purity of the samples was checked on precoated TLC plates (silica gel).

1.4.1 Detection of compounds on TLC technique

TLC plates were viewed under UV light at 254 nm for fluorescence quenching spots and at 356 nm for fluorescent spots. Anisaldehyde - sulfuric acid reagent was used as spraying reagent to detect the spots. (Pirrung. 2007) This reagent produced a variety of colors for different substances.

1.4.2 Column chromatography (CC)

Column chromatography was performed on a glass column packed with silica gel of particle size 230-400 mesh or Sephadex LH-20. The sample will be dissolved in a small volume of suitable organic solvent. The solution will be mixed with silica gel particle size < 0.063 mm or 0.040-0.063 mm, depending on the type of silica gel in column. The sample solution will be evaporated under reduced pressure and added onto the top of column. After loading of sample onto the column, and appropriate solvent system will be used as a mobile phase in the isocratic or gradient systems.

2. Synthesis of **hydroxyxanthone derivatives**

2.1 Synthesis of 1-hydroxyxanthen-9-one (30)

A mixture of resorcinol (1.154 g, 10.4 mmol), anhyd. $ZnCl_2$ (1 g, 7.3 mmol) and salicylic acid (1.340 g, 9.7 mmol) was heated at 180 °C in an oil bath for 6 h. After cooling, EtOAc (50 mL) was added to dissolve the reaction mixture, followed by silica gel (5 g) was added. Evaporation of the mixture to dryness afforded a dark red residue which was purified by column chromatrography (using 1% EtOAc-hexane as eluting system) to yield 1-hydroxyxanthen-9-one (**30**) as a pale yellow solid (1.59 g, 7.5 mmol, 71 % yield), $R_f$ 0.62 (30% acetone-hexane) and m.p. 145-146 °C (lit. 142-144°C, Coelho; et al. 2001: 117-123) (Coelho; et al. 2001: 117-123).

$^1$H NMR [DMSO-$d_6$] δ: 12.53 (s, 1H, 1-OH), 8.15 (dd, *J* = 7.9, 1.5 Hz, 1H, H-8), 7.90 (ddd, *J* = 8.4, 7.1, 1.5 Hz, 1H, H-6), 7.72 (t, *J* = 8.2 Hz, 1H, H-3), 7.64 (d, *J* = 8.4 Hz, 1H, H-5), 7.49 (t, *J* = 7.5 Hz, 1H, H-7), 7.06 (d, *J* = 8.4 Hz, 1H, H-4), 6.81 (d, *J* = 8.2 Hz, 1H, H-2)

$^{13}$C NMR [DMSO-$d_6$] δ: 181.7 (C-9), 160.9 (C-1), 155.7 (C-4a), 155.6 (C-10a), 137.5 (C-3), 136.5 (C-6), 125.4 (C-8), 124.6 (C-7), 119.8 (C-8a), 118.0 (C-5), 110.2 (C-2), 108.3 (C-9a), 107.2 (C-4),

MS: (ESI, +ve) *m/z*: 213.2 $[M+H]^+$ (100) for $C_{13}H_8O_3$

IR $\nu_{max}^{KBr}$ cm$^{-1}$: 2924, 2853, 1648, 1611, 1479, 1461, 1376, 1348, 1332, 1285, 1233, 1213, 1159, 1116, 1048, 1021, 931, 862, 816, 770, 725

2.2 Synthesis of 1,3-dihydroxyxanthen-9-one (31)

A freshly prepared methanesulfonic acid (36.5 g, 25 mL, 0.4 mol) was placed in a two-necked flask (500 mL) fitted with an efficient magnetically stirrer and a calcium chloride drying tube. Phosphorus pentoxide (3.6 g, 25.4 mmol) was added in one portion which was generally dissolved in 1-2 h. The reagent could be used immediately or could be stored in a stoppered flask for later use (Eaton; Carlson; & Lee. 1973: 4071-4073). Then the solution was added a mixture of phloroglucinol (1.262 g, 10.0 mmol) and salicylic acid (1.345 g, 9.7 mmol) and heated at 80 °C for 30 min. The reaction progress was monitored by TLC. After completion, the reaction mixture was poured into ice-water. The resulting orange solid was collected by

filtration, washed with water, dried in air, and the residue was then purified by column chromatography (using 10% acetone-hexane as eluting system ) to give a yellow crystal of the desired product (**31**, 1.590 g, 6.9 mmol, 71 % yield), $R_f$ 0.50 (30% acetone-hexane) and m.p. 254-255 °C (lit. 255-256 °C, Fotie; et al. 2003: 683-688) (Pillai; et al. 1986: 717-723).

$^1$H-NMR [acetone-$d_6$] δ: 12.89 (s, 1H, 1-OH), 8.16 (dd, *J* = 8.1, 1.6 Hz, 1H, H-8), 7.81 (ddd, *J* = 8.6, 7.1, 1.6 Hz, 1H, H-6), 7.50 (dd, *J* = 7.1, 0.9 Hz, 1H, H-5), 7.43 (ddd, *J* = 8.6, 8.1, 0.9 Hz, 1H, H-7), 6.41 (d, *J* = 2.0 Hz, 1H, H-4), 6.25 (d, *J* = 2.0 Hz, 1H, H-2)

$^{13}$C-NMR [acetone-$d_6$] δ: 181.2 (C-9), 166.6 (C-3), 164.7 (C-1), 158.8 (C-4a), 94.8 (C-2), 156.8 (C-10a), 136.1(C-6), 126.2 (C-8), 125.0 (C-7), 121.2 (C-8a), 118.46 (C-5), 103.7 (C-9a),99.0 (C-4)

MS (ESI, -ve): *m/z* 227.6 $[M-H]^-$(100) for $C_{13}H_8O_4$

IR $\nu_{max}^{KBr}$ cm$^{-1}$: 3394, 2925, 1654.2, 1610, 1457, 1352, 1312, 1284, 1223, 1193, 1164, 1077, 929, 855, 828, 788, 763, 727, 670, 600

**2.3 Synthesis of 1,6-dihydroxyxanthen-9-one (32) and 1,8-dihydroxyxanthen-9-one (33)**

Compounds **32** and **33** were synthesized by using the same procedure as described for compound **31** from resorcinol (612 mg, 5.5 mmol) and 2,6-dihydroxybenzoic acid (804 mg, 5.2 mmol) (Figure 15). The residue was purified by column chromatography (using 10% acetone-hexane as eluting system) to give a yellow solid of **32** (130.5 mg, 0.57 mmol, 10 % yields), $R_f$: 0.3 (30% acetone-hexane), m.p. 236-238 °C (lit. 246-248.5 °C, Fletcher; & Marlow. 1970: 937-939) and a yellow solid of **33** (21.4 mg, 0.1 mmol, 2 % yield), $R_f$ 0.37 (30% acetone-hexane), m.p. 190-191°C (lit. 192-194 C°, Fletcher; & Marlow. 1970: 937-939).

1,6-dihydroxyxanthen-9-one (**32**)

$^1$H-NMR [DMSO-$d_6$] δ: 12.82 (s, 1H,1-OH), 8.01 (d, *J* = 8.8 Hz, 1H, H-8), 7.64 (t, *J* = 8.3 Hz, 1H, H-3), 7.03 (d, *J* = 8.4 Hz, 1H, H-4), 6.92 (dd, *J* = 8.8, 2.1Hz, 1H, H-7), 6.75 (d, *J* = 8.2 Hz, 1H, H-2), 6.85 (d, *J* = 2.1 Hz, 1H, H-5)

$^{13}$C-NMR [DMSO-$d_6$] δ: 180.6 (C-9) 165.0 (C-6), 161.0 (C-1), 157.8 (C-10a), 155.0 (C-4a), 136.7 (C-3), 127.5 (C-8), 114.5 (C-5), 112.4 (C-9a), 110.1 (C-2), 107.3 (C-8a), 106.9 (C-7), 102.0 (C-4)

MS (ESI, -ve) *m/z*: 227.6 $[M-H]^-$(100) for $C_{13}H_8O_4$

IR $\nu_{max}^{KBr}$ cm$^{-1}$: 3513, 3085, 2343, 1642, 1523, 1481, 1388, 1328, 1226, 1187, 1118, 1069, 1049, 924, 853, 801, 764, 722, 687, 671, 604, 489

1,8-dihydroxyxanthen-9-one (**33**)

$^1$H-NMR [$CDCl_3$] δ: 11.80 (s, 2H,1-OH & 8-OH), 7.58 (t, *J* = 8.3 Hz, 2H, H-6 & H-3), 6.88 (d, *J* = 8.3 Hz, 2H, H-4 & H-5), 6.76 (d, *J* = 8.3 Hz, 2H, H-2 & H-7)

$^{13}$C-NMR [$CDCl_3$] δ: 186.2 (C-9), 161.3 (C-1 & C-8), 156.2 (C-4a & 10a), 137.1 (C-6 & C-3), 110.7 (C-7 & C-2), 110.7 (C-2), 107.1 (C-9a & C-8a), 106.7 (C-4 & C-5)

MS (ESI, -ve) *m/z*: 227.7 $[M-H]^-$ (100) for $C_{13}H_8O_4$

IR $\nu_{max}^{KBr}$ cm$^{-1}$: 3513, 3085, 2343, 1642, 1523, 1481, 1388, 1328, 1226, 1187, 1118, 1069, 1049, 924, 853, 801, 764, 722, 687, 671, 604

**2.4 Synthesis of 1,3,6-trihydroxyxanthen-9-one (34)**

Compound **34** was synthesized by using the same procedure as described for compound **31** from phloroglucinol (454.0 mg, 2.9 mmol) and the 2,4-dihydroxybenzoic acid (348 mg, 2.7 mmol). The mixture was purified by column chromatography (using 20-30% acetone-hexane as elute) to give a yellow solid of **34** (430 mg, 1.7 mmol, 60 % yield), $R_f$ 0.37 (30% acetone-hexane as eluting system) and decomposes at 260 °C (lit decomp. 332 °C, Lund; Robertson; & Whalley. 1953: 2434-2439.).

$^1$H-NMR [DMSO-$d_6$] δ: 13.04 (s, 1H, 1-OH), 10.54 -11.43 (br s, 1H, 6-OH, 3-OH), 7.95 (d, *J* = 8.7 Hz, 1H, H-8), 6.87 (d, *J* = 8.3 Hz, 1H, H-7), 6.80 (s, 1H, H-5), 6.33 (s, 1H, H-4), 6.15 (s, 1H, H-2),

$^{13}$C-NMR [DMSO-$d_6$] δ: 179.1 (C-9), 165.1 (C-3), 164.2 (C-6), 162.8 (C-1), 157.4 (C-10a) , 157.3 (C-4a), 127.2 (C-8), 114.0 (C-7), 112.3 (C-8a), 102.0 (C-5), 101.6 (C-9a), 97.9 (C-2), 93.9 (C-4)

MS (ESI, -ve) *m/z*: 243.7 $[M-H]^-$ (100) for $C_{13}H_8O_5$

IR $\nu_{max}^{KBr}$ $cm^{-1}$: 3394, 2925, 1654.2, 1610, 1457, 1352, 1312, 1284, 1223, 1193, 1164, 1077, 929, 855, 828, 788, 763, 727, 670, 600

### 2.5 Synthesis of 1,3,8-trihydroxyxanthen-9-one (35)

Compound **35** was synthesized by using the same procedure as described for compound **31** from phloroglucinol (1.261 g, 10.0 mmol) and the 2,6-dihydroxybenzoic acid (1.54 g, 10.0 mmol), and purified by column chromatography (using 20-30% acetone-hexane as eluting system) to give a yellow solid of **35** (871 mg, 3.3 mmol, 36 % yield), $R_f$ 0.37 (30% acetone-hexane) and m.p. 270-272 °C (lit 269-270°C, Fonteneau; et al. 2001: 9131-9135).

$^1$H NMR : [DMSO-$d_6$] δ: 11.83 (s, 1H, 8-OH), 11.76 (s, 1H, 1-OH), 7.65 (t, *J* = 8.4 Hz, 1H, H-6), 6.95 (d, *J* = 8.4 Hz, 1H, H-5), 6.75 (d, *J* = 8.1 Hz, 1H, H-7), 6.35 (d, *J* = 2.1 Hz, 1H, H-4), 6.20 (d, *J* = 2.1 Hz, 1H, H-2)

$^{13}$C NMR [DMSO-$d_6$] δ: 183.4 (C-9), 166.6 (C-3), 162.2 (C-1), 160.3 (C-8), 157.5 (C-4a), 155.5 (C-10a), 137.2 (C-7), 110.6 (C-5), 107.1 (C-6), 106.9 (C-8a), 101.1 (C-9a), 98.6 (C-2), 94.4 (C-4)

MS : (ESI, -ve) *m/z* : 243.9 $[M-H]^-$ (100) for $C_{13}H_8O_5$

IR $\nu_{max}^{KBr}$ $cm^{-1}$: 3512, 3087, 2343, 1609, 1478, 1277, 1226, 1160, 1117, 1048, 924, 801, 764, 670

### 2.6 Synthesis of 1,3,6,8-tetrahydroxyxanthen-9-one (36)

Compound **36** was synthesized by using the same procedure as described for compound **31** from phloroglucinol (1.261 g, 10 mmol) and 2,4,6-trihydroxybenzoic acid (**35**, 1.70 g, 10.0 mmol), and the residue was then purified by flash column chromatography (using 20-30% acetone-hexane as eluting system) to give a yellow solid of **36** (836 mg, 3.2 mmol, 32 %

yield), $R_f$ 0.30 (40% acetone-hexane) and m.p. 343-345 °C (lit. 347-348 °C, Fotie ; et al. 2003: 683-688).

$^1$H-NMR [DMSO-$d_6$] δ: 11.89 (s, 2H, 8-OH & 1-OH) , 6.30 (s, 2H, H-5 & H-4), 6.15 (s, 2H, H-7 & H-2)

$^{13}$C-NMR [DMSO-$d_6$] δ: 182.0 (C-9), 165.8 (C-6 & C-3), 162.0 (C-8 & C-1), 157.2 (C-4a), 157.1 (C-10a), 100.4 (C-9a & C-8a), 94.3 (C-5 & C-4), 98.4 (C-7 & C-2)

MS (ESI, -ve) *m/z* : 259.6 $[M-H]^-$ (100) for $C_{13}H_8O_6$

IR $\nu_{max}^{KBr}$ cm$^{-1}$: 3530, 3084, 2882, 2817, 2735, 2652, 1640, 1616, 1524, 1461, 1385, 1321, 1279, 1184, 1159, 1116, 1085, 1069, 1009, 978, 927, 833, 759

**3. Prepration of mangosteen pericarp extracts**

The mangosteen fruit (1 kg) was bought from Minburi market, Bangkok, Thailand, in November, 2012. The fresh pericarps were cleaned and the edible aril parts and caps were removed. The fruit pericarps were cut into small pieces (2 cm) and dried in a hot oven at 60 ºC for 24 h. to yield the dried brown pericarp (430 g).

**3.2 Prepration of mangosteen extract by different solvents**

3.2.1 Extration with water

The dried pericarp (20 g) was extracted with reverse osmosis water or RO water (2x160 ml) at 60 ºC for 2 h. The supernatant was concentrated under reduced pressure at 40 °C by a rotary evaporator and MeOH (2x20 ml) was added and filtered through a Whatman filter paper (no. 1) (to remove pectin). The filtrate was evaporated to dryness by a rotary evaporator and was then freeze-dried to give an extract (**E1**) as a red solid (2.25 g, 11 % base on dried pericarp).

3.2.2 Extraction with ethanol

The dried pericarp of mangosteen (20 g) was extracted with 95 % ethanol (2 x 160 ml) at room temperature for 24 h. The supernatant was filtered through a Whatman filter paper (no. 1) and concentrated under reduced pressure at 40 °C by a rotary vacuum evaporator until

dryness to give an ethanol extract (**E2**) as a yellow-brown solid (2.75 g, 13 % base on dried pericarp).

3.2.3 Extraction with acetone

By using the same method as described for the ethanol extraction, but using acetone in place of ethanol. The filtrate was evaporated under vacuum at 40 °C to dryness to give an acetone extract (**E3**) as a yellow-brown solid (2.52 g, 12 % base on dried pericarp).

3.2.4 Extraction with 60% ethanol-water

The 60 % ethanol-water extract from dried pericarp of mangosteen (20 g) was extracted by using the same method as described for the ethanol extraction. The filtrate was evaporated in vacuum at 40 °C to dryness to give an ethanol-water extract (**E4**) as a red-brown solid (2.02 g, 10 % base on dried pericarp).

A portion of the extract (1.20 g) was subjected to liquid–liquid extraction with $CH_2Cl_2$ (3 ×50 ml) and water (3x50 ml). Both phases were pulled and concentrated to dryness to give a $CH_2Cl_2$ (**E5**) and aqueous (**E6**) fractions as yellow (0.52 g) and red (0.72 g) solids, respectively.

3.2.5 Extraction with 60% acetone-water

The 60 % acetone-water extract from dried pericarp of mangosteen (20 g) was extracted by using the same method as described for the 60% ethanol-water. The filtrate was evaporated in vacuum at 40 °C to dryness to give an ethanol-water extract (**E7**) as a red-brown solid (1.61 g, 8 % base on dried pericarp).

**4. CFTR inhibitory activity evaluation**

The tested samples were screened at for effects on cAMP-activated $Cl^-$ secretion across a monolayer of human crypt-like epithelial T84 cells and Fisher rat thyroid (FRT) cells by short circuit current analysis (Department of Physiology, Faculty of Science, Mahidol University) (Luerang et al. 2012; 988-994).

# CHAPTER 4
# RESULTS AND DISCUSSION

## 1. Synthesis of hydroxyxanthone derivatives and evaluation of their CFTR inhibitory activity

Hydroxyxanthones (**30-36**) have been designed and synthesized by using an oxidative coupling reaction of the corresponding *o*-hydroxybenzoic acids and activated phenols. 1-Hydroxyxanthone (**30**) was synthesized in 71% yield by heating at 180 °C for 8 h. as desenbed previously of a mixture between salicylic acid and resorcinol under anh. $ZnCl_2$ catalysis. Xanthones **31** and **34-36** were prepared in 32-71% yield by using a similar manner from different hydroxybenzoic acids and phloroglucinol but using a freshly prepared mixture of methanesulfonic acid and $P_2O_5$ in place of $ZnCl_2$ under heating at 80 °C. Compounds **32** and **33** were obtained in 10 and 2 % yields, respectively, by using the same procedure as described for **30** from resorcinol and 2,6-dihydroxybenzoic acid. Schematic synthesis of these xanthones was depicted in Figure 15. The structures of these compounds were confirmed mainly by NMR (1D- and 2D-NMR) and MS techniques. Spectroscopic data of **30-36** were in agreement with the structures and were consistent with the literature values (Pillai et al. 1985; 717-723).

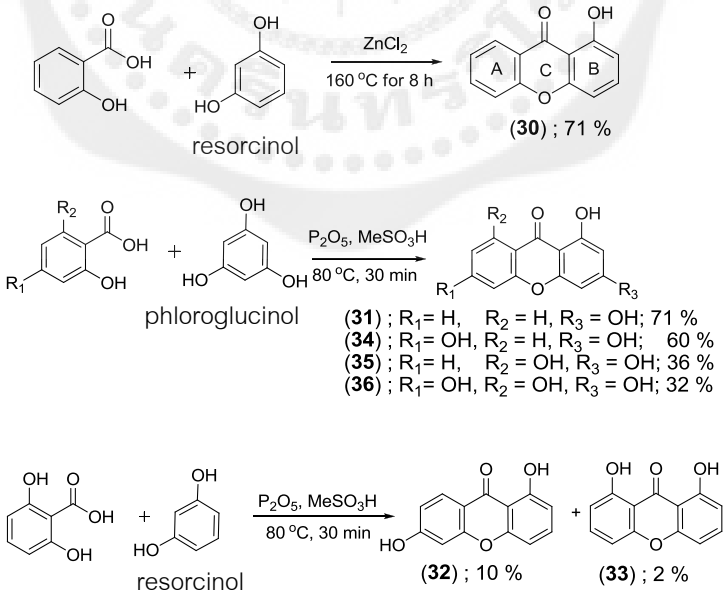


Figure 15 Synthesis of hydroxyxanthene-9-one derivatives **30-36**

The reaction mechanism proceeds via an oxidative coupling reaction as shown in Figure 16. Polyphosphoric acid (PPA) is formed by interaction of $P_2O_5$ with $CH_3SO_3H$ (Ying-Hung So and Jerry P. Heeschen 1997; 3352-3561). Protonation on 2,4-dihydroxybenzoic by PPA leads to benzoyl cation intermediate formation. Coupling reaction of phloroglucinol with the cation giving a benzophenone, followed by cyclization and dehydration gives the target xanthone **34**.

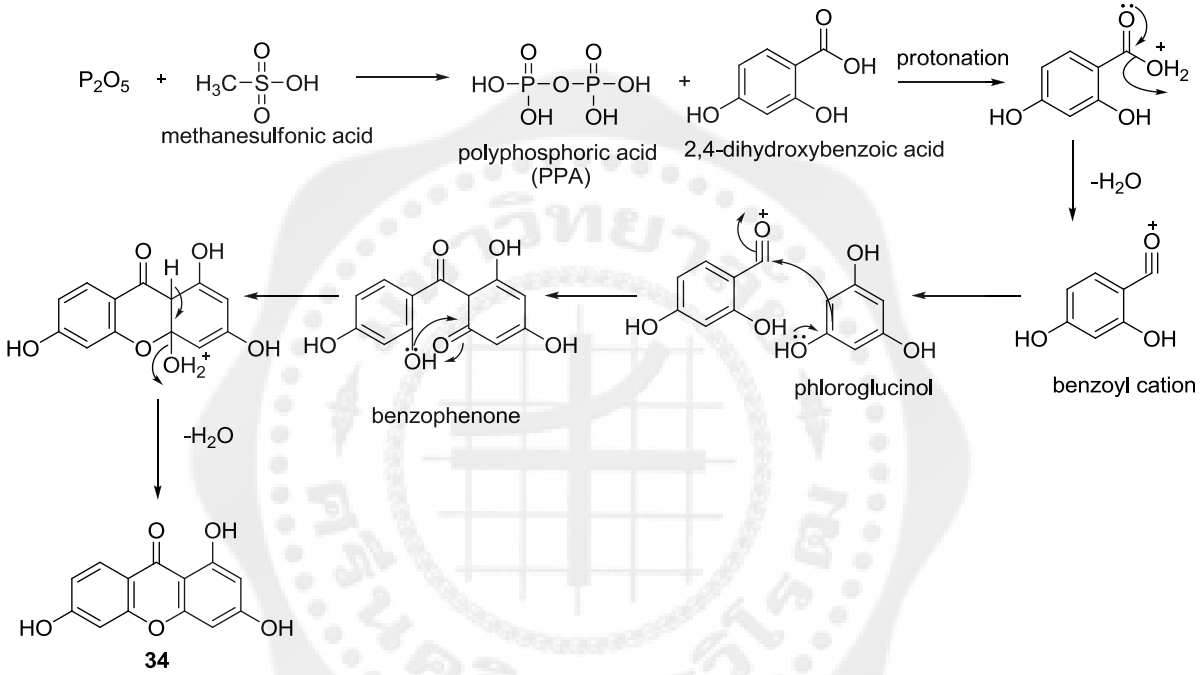


Figure 16 Proposed mechanism for hydroxyxanthone formation via oxidative coupling

### 1.1 1-hydroxyxanthen-9-one (30)

Compound **30** showed a base peak at *m/z* 213.2 $[M+H]^+$ in its ESIMS spectrum which coresponed to a molecular formula of $C_{13}H_8O_3$. Its $^1$H-NMR spectrum showed a highly singlet at $\delta$ 12.53 in the downfield region, which corresponded to the presence of a chelated hydroxyl proton of C-1. The aromatic protons showed signals for a doublet of doublet at $\delta_H$ 8.16 ($J$ = 7.9, 1.5 Hz, H-8), a doublet of doublet of doublet at $\delta_H$ 7.90 ($J$ = 8.4, 7.1, 1.5 Hz, H-6), two triplets at $\delta_H$ 7.72 ($J$ = 8.3 Hz, H-3), 7.49 ($J$ = 7.5 Hz, H-7) and three doublets at $\delta_H$ 7.64 (H-5, $J$ = 8.4 Hz), 7.06 (H-4, $J$ = 8.2 Hz ) and 6.81 (H-2, $J$ = 8.2 Hz). The $^{13}$C-NMR spectrum showed thirteen carbon signals in the region of 107.2-181.7. Among these carbon signals, the peak with the

highest chemical shift at $\delta_C$ 181.7 corresponded to conjugated carbonyl carbon, others corresponded to 5 quaternary carbons, and 6 methine carbons. The assignments of carbon signals above were carried out based on HMQC and HMBC spectral data analysis. The quaternary carbon at $\delta_{C\text{-}1}$ 160.9 and methine proton of H-2 and H-3 signals confirmed the hydroxyl group was placed at C-1 in ring B of xanthone nucleus (Figure 19).

**1.2 1,3-dihydroxyxanthene-9-one (31)**

Compound **31** showed *m/z* 277.6 $[M\text{-}H]^-$ in its ESIMS spectrum which coresponed to a molecular formula of $C_{13}H_8O_4$. Its $^1$H-NMR data at ring A of showed similar pattern to that of compound **30**, except for H-4 and H-2 in **31** showed doublet of doublet at $\delta_H$ 6.41 and 6.25, respectively, with a *meta* coupling constant 2.0 Hz. A HMBC correlation was observed between the methine proton signal of H-4 and a quaternary carbon at $\delta$ 166.6 (C-3) confirmed the hydroxyl group was placed at C-3 in ring B of xanthone nucleus (Figure 20).

**1.3 1,6-dihydroxyxanthen-9-one (32)**

Compound **32** showed *m/z* 277.6 $[M\text{-}H]^-$ in its ESIMS spectrum which coresponed to a molecular formula of $C_{13}H_8O_4$. Its $^1$H-NMR data at ring B of showed similar pattern to that of compound **30**. A typical AMX spin system for H-8 (d, *J* = 8.8), H-7 (dd, *J* = 8.8, 2.1 Hz) and H-5 (d, *J* = 2.1 Hz, 1H, H-5) was observed in its $^1$H-NMR data. In addition, a long-range $^{13}$C-$^1$H coupling between the quaternary carbon at $\delta$ 165.0 (C-6) and methine proton of H-8 and H-5 signals confirmed the hydroxyl group was placed at C-6 in ring A of xanthone nucleus (Figure 21).

**1.4 1,8-dihydroxyxanthen-9-one (33)**

Compound **32** showed *m/z* 277.6 $[M\text{-}H]^-$ in its ESIMS spectrum which coresponed to a molecular formula of $C_{13}H_8O_4$. Its $^1$H-NMR data of showed two chelated hydroxyl protons at $\delta_H$ 11.79, triplet proton at $\delta_H$ 7.58 (*J* = 8.3 Hz, H-3 and H-6), four doublet protons at $\delta_H$ 6.87 (*J* = 8.3 Hz, H-4 and H-5) and $\delta_H$ 6.76 (*J* = 8.3 Hz, H-2 and H-7). Quaternary carbon of C-1 and C-8 at

$\delta_C$ 161.3 showed correlations with 1- and 8-hydroxyproton ($\delta_H$ 11.79) confirmed the hydroxyl group was placed at C-3 and C-8 of xanthone nucleus (Figure 22).

**1.5 1,3,6-trihydroxyxanthen-9-one (34)**

Compound **34** showed *m/z* 243 $[M-H]^-$ in its ESIMS spectrum which coresponed to a molecular formula of $C_{13}H_8O_5$. Its $^1$H-NMR spectrum showed the aromatic protons similar to that of compound **32** in ring A. In addition, H-2 and H-4 were exhibited two siglets at $\delta_H$ 6.33 and 6.15, respectively. In HMBC spectrum, quaternary carbon at $\delta$ 164.2 (C-6) showed correlations at $\delta$ 6.87 (H-7), 6.80 (H-5) and 7.95 (H-8). Moreover, quaternary carbon of C-3 at $\delta_C$ 165.1 also showed correlations with $\delta_{H-4}$ 6.33 and $\delta_{H-2}$ 6.15, that confirmed the structure for 1,3,6-trihydroxyxanthen-9-one (Figure 23).

**1.6 1,3,8-trihydroxyxanthen-9-one (35)**

Compoud **35** showed *m/z* 243.7 $[M-H]^-$ in its ESIMS spectrum which coresponed to a molecular formula of $C_{13}H_8O_5$. Its $^1$H-NMR spectrum at ring B showed the aromatic protons similar to that of compound **31**. The aromatic proton of ring A exhibited a triplet at $\delta_H$ 7.65 (*J* = 8.4 Hz, H-6) and two doublets at $\delta_H$ 6.95 (*J* = 8.4 Hz, H-5) and 6.75 (*J* = 8.1 Hz, H-7). Quaternary carbon of C-8 at $\delta_C$ 160.3 showed correlations with 8-hydroxy proton ($\delta_H$ 11.76) and three protons of H-5, 7 and 6 in HMBC spectrum. In addition, the HMBC correlation of quaternary carbon at $\delta$ 166.6 (C-3) with H-4 ($\delta_H$ 6.35) and H-2 ($\delta_H$ 6.20) confirmed the hydroxyl group was placed at C-3 in xanthone nucleus (Figure 24).

**1.6 1,3,6,8-tretrahydroxyxanthen-9-one (36)**

Compound **36** showed *m/z* 259.6 $[M-H]^-$ in its ESIMS spectrum which coresponed to a molecular formula of $C_{13}H_8O_6$. Its $^1$H-NMR spectrum of compound **36** showed two chelated hydroxyl protons similar as a compound **33**. The aromatic proton showed two singlets at $\delta_H$ 6.30 (2H, H-4 and H-5) and 6.15 (2H, H-2 and H-7). Quaternary carbon of C-1 and C-8 displayed the same chemical shift at $\delta_C$ 162.0 showed the HMBC correlations with the OH-1 and OH-8 groups

at $\delta_H$ 11.88. Moreover, C-3 and C-6 at $\delta_C$ 165.8 exhibited the correlations with H-4 and 5 in its HMBC spectrum confirmed the structure (Figure 25).

All synthesized compounds **30-36** including a commercially available non-hydroxylated xanthone **29** were evaluated for CFTR inhibitory activity on human intestinal epithelial (T84) cell and FRT cells by short circuit current analysis. It was found that at concentration 100 $\mu$M of **29-36** inhibited on db-cAMP-induced $Cl^-$ secretion by 5, 8, 12, 16, 20, 52, 30 and 42 %, respectively, as shown in Table 1. Among the compound tested, 1,3,6-trihydroxyxanthen-9-one (**34**) was the highest activity with 52 % inhibition. The presence of the hydroxyl groups at positions 1, 3 and 6 on xanthone scaffold in **34** was crucial for increasing inhibitory activity, as compared with those on other positions of the monohydroxylation (as in 1-hydroxyxanthone, **30**), dihydroxylation (as in 1,3-, 1,6- and 1,8-dihydroxyxanthones, **31-33**), trihydroxylation (as in 1,3,8-trihydroxyxanthone, **35**), and tetrahydroxylation (as in 1,3,6,8-tetrahydroxyxanthone, **36**), including the non-hydroxylated compounds **29**.

Table 1. The percent of CFTR inhibition ($\mu$M) of compounds **29-36**

| Structure | % CFTR inhibition at 100 $\mu$M | $IC_{50}$ ($\mu$M) | Structure | % CFTR inhibition at 100 $\mu$M | $IC_{50}$ ($\mu$M) |
|---|---|---|---|---|---|
| 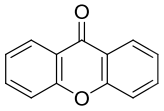 **29** | 5 | >500 | 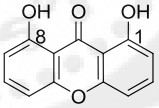 **33** | 20 | 200-500 |
| 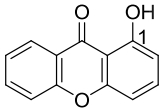 **30** | 8 | >500 | 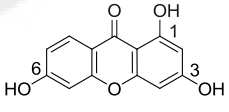 **34** | 52 | ~100 |
| 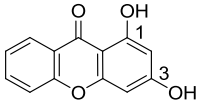 **31** | 12 | >500 | 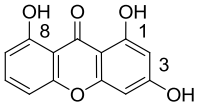 **35** | 30 | 100-200 |
| 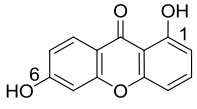 **32** | 16 | >500 | 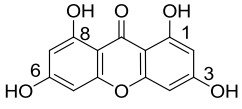 **36** | 42 | ~100 |

Therefore, 1,3,6-trihydroxyxanthen-9-one (**34**) was selected for characterization for its mechanisms of action as well as potential application in the anti-secretory therapy for cholera. Dose-inhibition study in T84 cell monolayer showed that compound **34** dose-dependently inhibited the db-cAMP induced $Cl^-$ secretion with an $IC_{50}$ of ~100 $\mu$M and complete inhibition at 500 $\mu$M (Fig 17A and 17B)

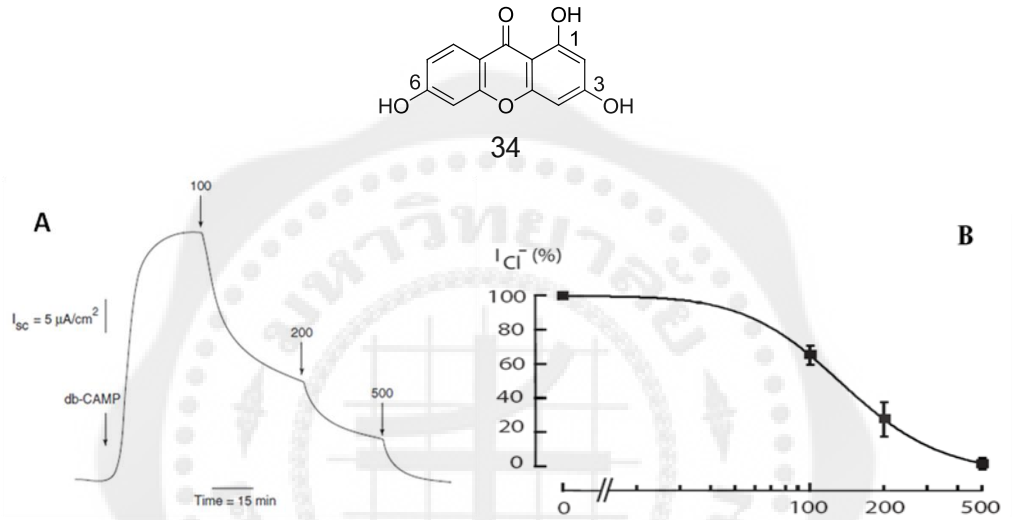


Figure 17 (A). Effect of 1,3,6-trihydroxyxanthone (**34**) on cAMP-activated $Cl^-$ by apical chloride current measurements in FRT-CFTR. (B). Dose-inhibition study in T84 cell monolayers showed that the most potent activity of compound **34** at 500 $\mu$M.

**2. Preparation of *G. mangostana* pericarp extracts and evaluation for their CFTR inhibitory activity**

Mangosteen or *G. mangostana* has long been used to treat diarrheal illness in traditional medicine (Pedraza-Chaverri 2008; 3227-3339). Flavonoids (**13-19**), tannin (**20**), oligomeric proanthocyanidin (**22-28**) including hydroxyxanthones (as described above) have been reported as CFTR inhibitors (**34**). Prenylated xanthones, tannin, anthocynin and proanthrocyanin are major chemicals found in pericarp (**14**). However, the effect of mangosteen pericarp extract on $Cl^-$ secretion has never been investigated. The present study was therefore conducted to investigate the effect of the extract on cAMP-activated $Cl^-$ secretion.

Mangosteen fruit is composed of 65% of pericarp, 31% of flesh and 4% of cap (Chaovanalikit et al.2012; 1047-1053). The dried pericarp without cap of *G. mangostana* was selected for extraction with different polar solvents of water, ethanol, acetone, 60% ethanol-water and 60% acetone-water. Five respective crude extracts (**E1**, **E2**, **E3**, **E4** and **E7**) were obtained as shown in Table 2. All crude extracts were submitted for CFTR inhibitory activity evaluations on T84 cell and FRT cells by short circuit current analysis. The results showed that at concentration 50 $\mu$g/ ml only the crude extract **E4** (60% ethanol-water) inhibited on db-cAMP-induced $Cl^-$ secretion by 60 % (Figure 18), where as other extracts were inactive under the same screening, as shown in table 2. Further investigation to search for the active component was performed. The active extract was thus fractionated with $CH_2Cl_2$-water to give a $CH_2Cl_2$ (**E5**) and an aqueous (**E6**) fractions and their 1H NMR spectra were depicted in figure 26 and 27, respectively. Unfortunately, both fractions were also inactive on cAMP-activated $Cl^-$ secretion screening. $^1$H-NMR data analysis of the $CH_2Cl_2$ fraction was proved to be a mixture of prenylated xanthones (Figure 26). $\alpha$-Mangostin, the major xanthone of mangosteen pericarp also found inactive under the same test, this could be accounted for inactivity of the $CH_2Cl_2$ fraction. Water soluble compounds like anthocynin and proanthrocyanin are also major chemicals found in fruit pericarp and have been reported as CFTR inhibitors. The inactivity of the aqueous phase, however, remained unclear at this stage. Further chemical investigation of the aqueous extract is recommended which might clarify for such inactivity.

Table 2. *G. mangostana* pericarp extracts and their CFTR inhibitory activity evaluations

| Extract | Appearance | Weight (%) | % inhibition |
|---|---|---|---|
| water extract (**E1**) | red solid | 2.25 g (11 %) | inactive |
| 95% ethanol extract (**E2**) | yellow-brown solid | 2.75 g (13 %) | inactive |
| acetone extract (**E3**) | yellow-brown solid | 2.52 g (12 %) | inactive |
| 60% ethanol-water extract (**E4**) | red-brown solid | 2.02 g (10 %) | 60 |
| - $CH_2Cl_2$ fraction (**E5**) | yellow solid | 0.52 g | inactive |
| - aqueous fraction (**E6**) | red solid | 0.72 g | inactive |
| 60% acetone-water extract (**E7**) | yellow-brown | 1.61 g (8 %) | inactive |

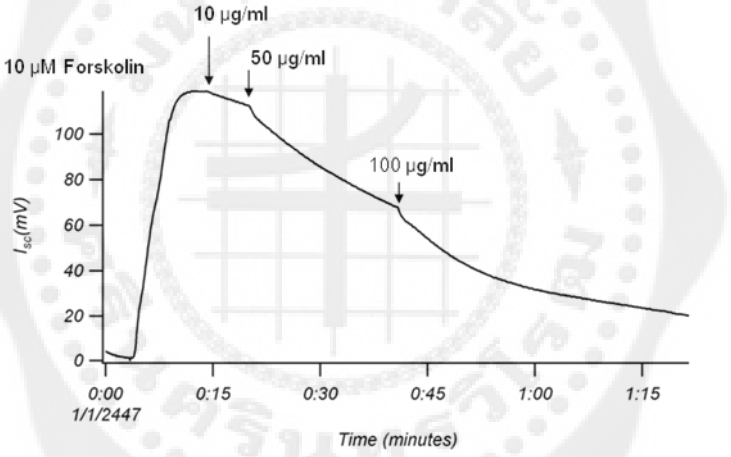


Figure 18 Effect of the 60% ethanol-water extract (**E4**) on cAMP-activated $Cl^-$ by apical chloride current measurements in FRT-CFTR.

# CHAPTER 5
# CONCLUSION

## 1. CFTR Inhibitory activity of hydroxyxanthen-9-one derivatives (30-36)

CFTR inhibitor is a target for treatment as anti-secretory diarrhea. In this study, a series of hydroxyxanthen-9-one derivatives (**30-36**) were synthesized in 2-71 % yields from an oxidative coupling reaction between the corresponding *o*-hydroxybenzoic acids and activated phenols. All synthesized compounds were evaluated as potential inhibitors of CFTR by short circuit current analysis. Among tested compounds, 1,3,6-trihydroxyxanthone (**34**) was the most effective CFTR inhibitor with 52 % inhibition at 100 $\mu$M and an $IC_{50}$ value of ~100 $\mu$M.

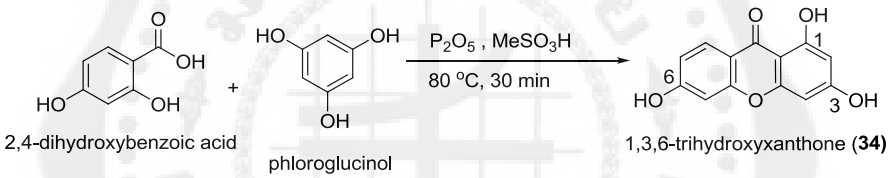


For the structure activity relationship study, the presence of the hydroxyl groups at positions 1, 3 and 6 on the xanthone scaffold in **34** was crucial for increasing inhibitory activity, as compared with other xanthones bearing hydroxyl groups on other positions. This is the first report on hydroxyxanthones act as CFTR inhibitor. Hydroxyxanthones represent another class of polyphenols which might be prospect for future development of pharmacotherapy for cholera.

## 2. CFTR inhibitory activity of extracts obtained from the dried pericarp of mangosteen

In Thai folk medicine, the dried fruit pericarp of *G. mangostana* has been long used for treating diarrhea. However, the effect of mangosteen pericarp extract on $Cl^-$ secretion has never been investigated. The present study was therefore conducted to investigate the effect of the mangosteen extract on cAMP-activated $Cl^-$ secretion. Thus five mangosteen pericarp extracts were prepared from the dried fruit pericarp by using different polarity of solvents. All crude

extracts were evaluated for CFTR inhibitory activity on T84 cell and FRT cells by short circuit current analysis. The results showed that at concentration 50 $\mu$g/ ml only the 60% ethanol-water extract (**E4**) inhibited on db-cAMP-induced $Cl^-$ secretion by 60 %, where as other extracts were inactive under the same screening. Following fractionating of the active extract with $CH_2Cl_2$-water system, unfortunately, the resulting $CH_2Cl_2$ and aqueous fractions were also inactive on cAMP-activated $Cl^-$ secretion screening.

# BIBLIOGRAPHY

# BIBLIOGRAPHY

Cai, Z., Scott-Ward, T., Li, H., and Schmidt, D. (2004). Strategies to investigate the mechanism of action of CFTR modulators. *Journal of Cystic Fibrosis*. 3: 141-147.

Chaovanalikit, A., Mingmuang, A., Kitbunluewit, T., Choldumrongkool, N., Sondee, J. and Chupratum, S. (2012). Anthocyanin and total phenolics content of mangosteen and effect of processing on the quality of mangosteen products. *International Food Research Journal* 19 (3): 1047-1053

Chin, Y., and Kinghorn, A. (2008). Structural characterization, biological effects, and synthetic studies on xanthones from mangosteen (*Garcinia mangostana*), a popular botanical dietary supplement. *Mini-Reviews in Organic Chemistry*. 5(4): 355-364.

Galietta, LJ., and Moran, O. (2004). Identification of CFTR activators and inhibitors: chance or design ?. *Current Opinion in Pharmacology*. 4: 497-503.

Gout, T. (2012). Role of ATP binding and hydrolysis in the gating of the cystic fibrosis transmembrane conductance regulator. *Annals of Thoracic Medicine*. 7(3): 115-121.

Hwang, T.C., and Sheppard, D.V. (1999). Molecular pharmacology of the CFTR $Cl^-$ channel. *Trend in Pharmacological Science*. 20: 448-453.

Pedraza-Chaverri , J., Cárdenas-Rodríguez, N.,Orozco-Ibarra, M., and Jazmin M. Pérez-Rojas (2008). Medicinal properties of mangosteen (Garcinia mangostana*). Food and Chemical Toxicology*. 46: 3227-3239

Link studio. (2014). Cystic fibrosis transmembrane conductance regulatorhttp. Retrived 2 3, 2014, from http://www.linkstudio.info/portfolio/illustration05.htm.

Luerang, W., Khammee, T., Kumpum, **W**., Suksamrarn, S., Chatsudthipong, V., Muanprasat, C. (2012). Hydroxyxanthone as an inhibitor of cAMP-activated apical chloride channel in human intestinal epithelial cell. *Life Sciences* 90: 988-994.

Ma, T., Thiagarajah, J.R., Yang, H., Sonawane, N.D., and Folli, C. (2002). Thiazolidinone CFTR inhibitor identified by high-throughput screening blocks cholera toxin-induced intestinal fluid secretion. *The Journal of Clinical Investigation.* 11: 1651- 1658.

Muanprasat, C., Sonawane, N.D., Salinas, S., Taddel, A., Galietta, L., and Verkman, A.S. (2004). Discovery of Glycine hydrazine pore-occluding CFTR inhibitor: mechanisim, structure-activity analysis, and in vivo efficacy. *The Journal of General Physiology.* 26: 125-137.

Patanayindee, J., Muanprasat, C., Soodvilai, S., and Chatsudthipong, V. (2012). Antidiarrheal efficacy of a quinazolin CFTR inhibitor on human intestinal epithelial cell and in mouse model of cholera. *Indian Journal of Pharmacology.* 44(5): 619-623.

Pedraza-Chaverri, J., Cárdenas-Rodríguez, N., Orozco-Ibarra, M., and Pérez-Rojas, J. (2008). Medicinal properties of mangosteen *(Garcinia mangostana). Food and Chemical Toxicology*. 46: 3227-3239.

Pillai, R., Naiksatam, P., Johnson, F., Rajagopalan, R., Watts, P., and Borras, S. (1986). Thermorubin II. 1,3-Dihydroxy-9H-xanthones and 1,3-dihydroxy-9H-xanthenes. New methods of synthesis. *Journal of Organic Chemistry.* 51: 717-723.

Ren, A., Zhang, W., Thomas, H.G., Barish, A.; Berry, S., Kiel, J.S., and Naren, A.P. (2012). A Tannic acid-based medical food, Cesinex®, exhibits broad-spectrum antidiarrheal properties: A mechanistic and clinical study. *Digestive Diseases and Science.* 57(1): 99-108.

Schuier, M., Sies, H., Lllek, B., and Fischer, H. (2005). Cocoa-related flavonoids inhibie CFTR-mediated chloride transport across T84 human colon epithelia. *The Journal of Nutrition*. 135(10): 2320-2325.

Thiagarajah, J.R., and Verkman, A.S. (2003). CFTR pharmacology and its role in intestinal fluid secretion. *Current Opinion Pharmacology*. 3: 594-599.

Thiagarajaha, J.R., and Verkman, A.S. (2005). New drug targets for cholera therapy. *Trends in Pharmacological Sciences*. 26: 172-174.

Verkman, A.S., Chaturvedi, P., Tradtrantip, L., and Namkung, W., inventors; Napo pharmaceuticals Inc, applicant. (2012 Aug 9). Methods of treating diseases with proanthocyanidin oligomers such as crofelemer. US patent 0202876.

Wongsamitkul, N., Sirianant, L., Muanprasat, C., and Chatsudthipong, V. (2010). Plant-derived hydrolysable tannin inhibits CFTR chloride channel: a potential treatment of diarrhea. *Pharmaceutical Research*. 27(3): 490-497.

Ying-Hung So and Jerry P. Heeschen. (1997). Mechanism of Polyphosphoric acid and phosphorus pentoxide-methanesulfonic acid as synthetic reagents for benzoxazole formation. *Journal of Organic Chemistry*. 62: 3352-3361

Zhang, W., Fujii, N., and Naren, A. (2012). Recent advances and new perspectives in targeting CFTR for therapy of cystic fibrosis and enterotoxin-induced secretory diarrheas. *Future Medical Chemistry*. 4(3): 329-345.

Zhiwei, C., Scott-Ward, T.S., Li, H., Schmidt, A., and Sheppard, D. (2004). Strategies to investigate the mechanism of action of CFTR modulators. *Journal of Cystic Fibrosis.* 3: 141-147.

# APPENDIXES

# APPENDIXES

NMR spectrum

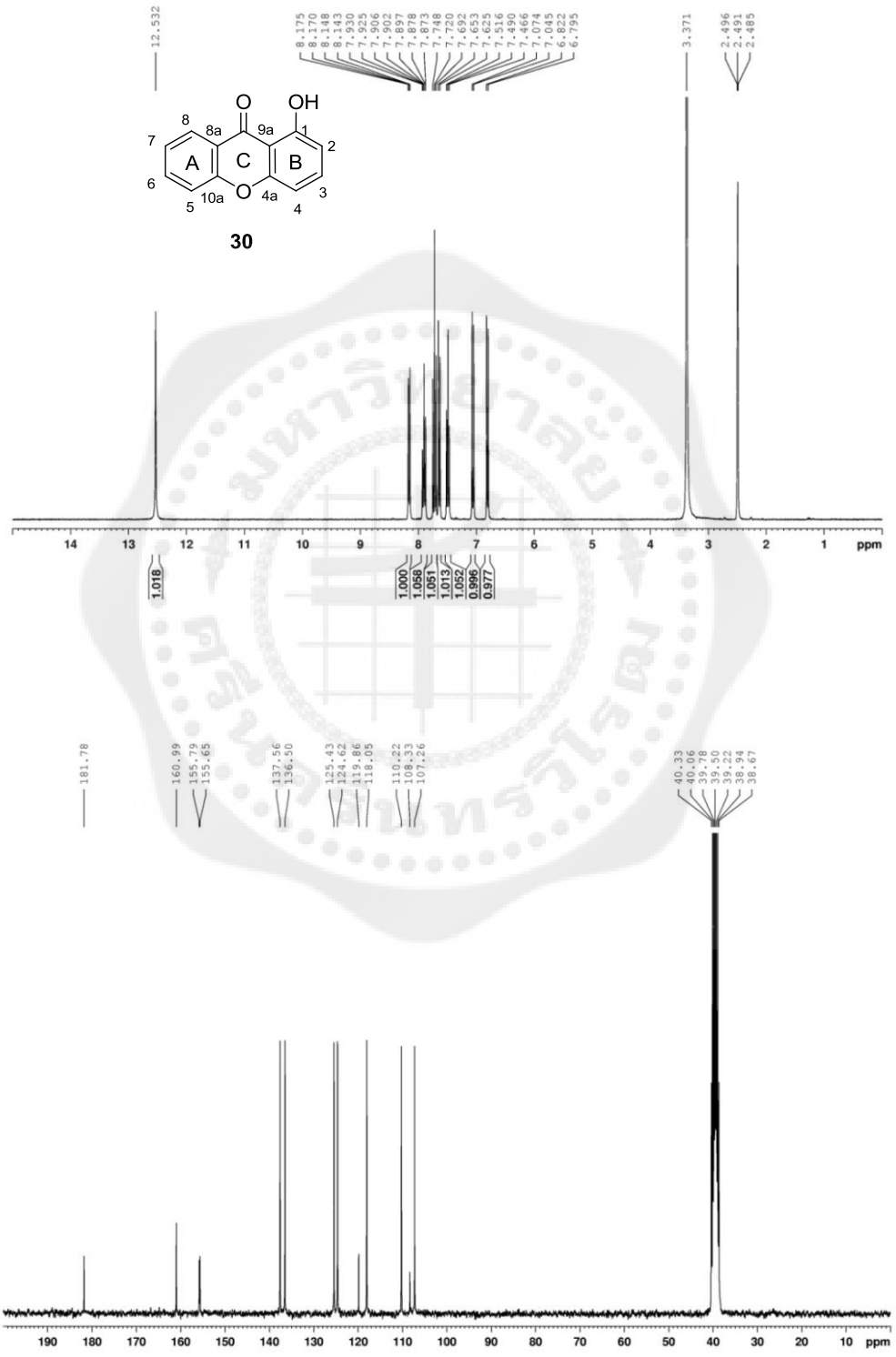


Figure 19 $^{1}$H- and $^{13}$C-NMR spectrum of 1-hydroxythioxanthen-9-one (**30**) in DMSO-$d_6$

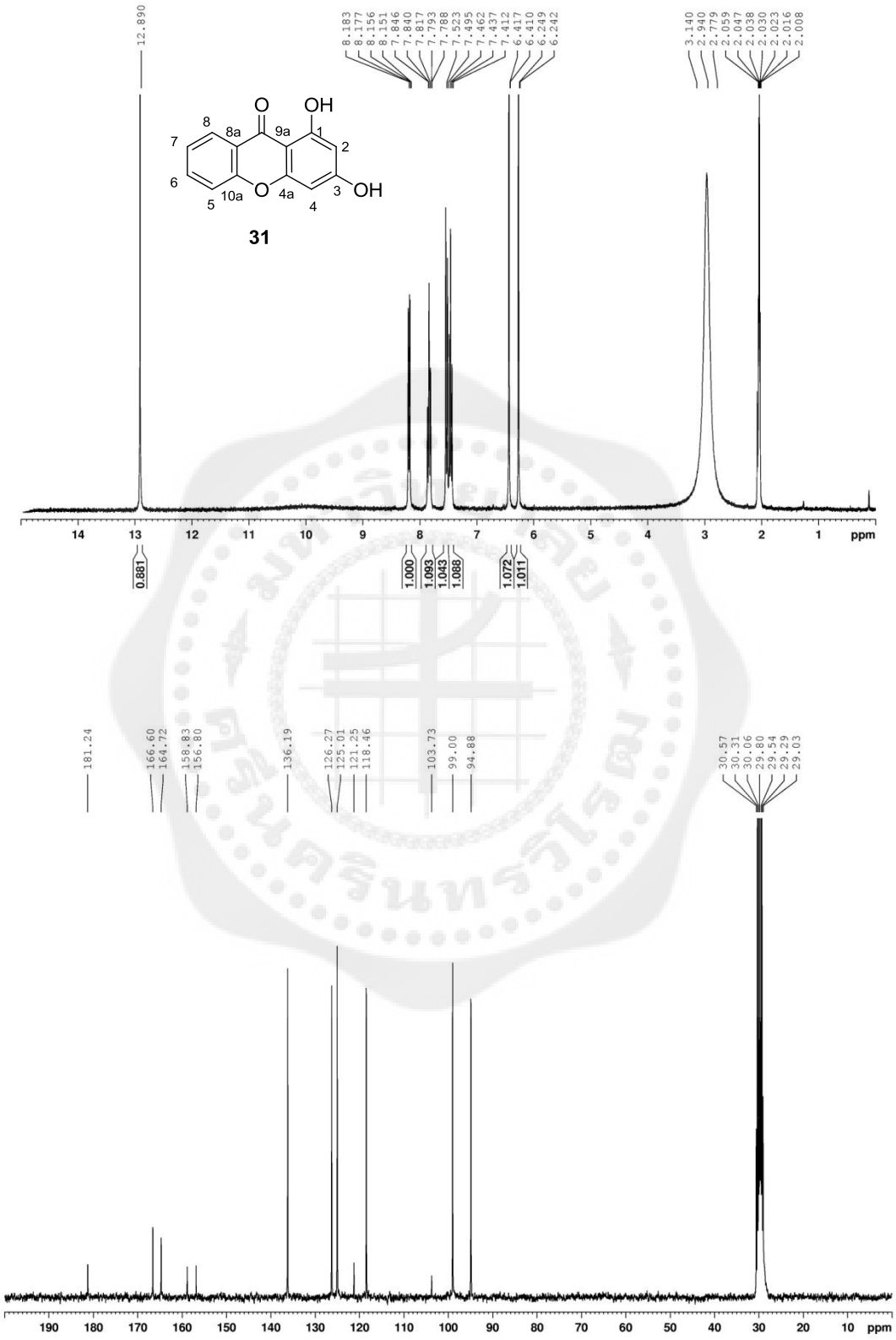


Figure 20 $^{1}$H- and $^{13}$C-NMR spectra of 1,3-dihydroxyxanthen-9-one (**31**) in Acetone-$d_6$

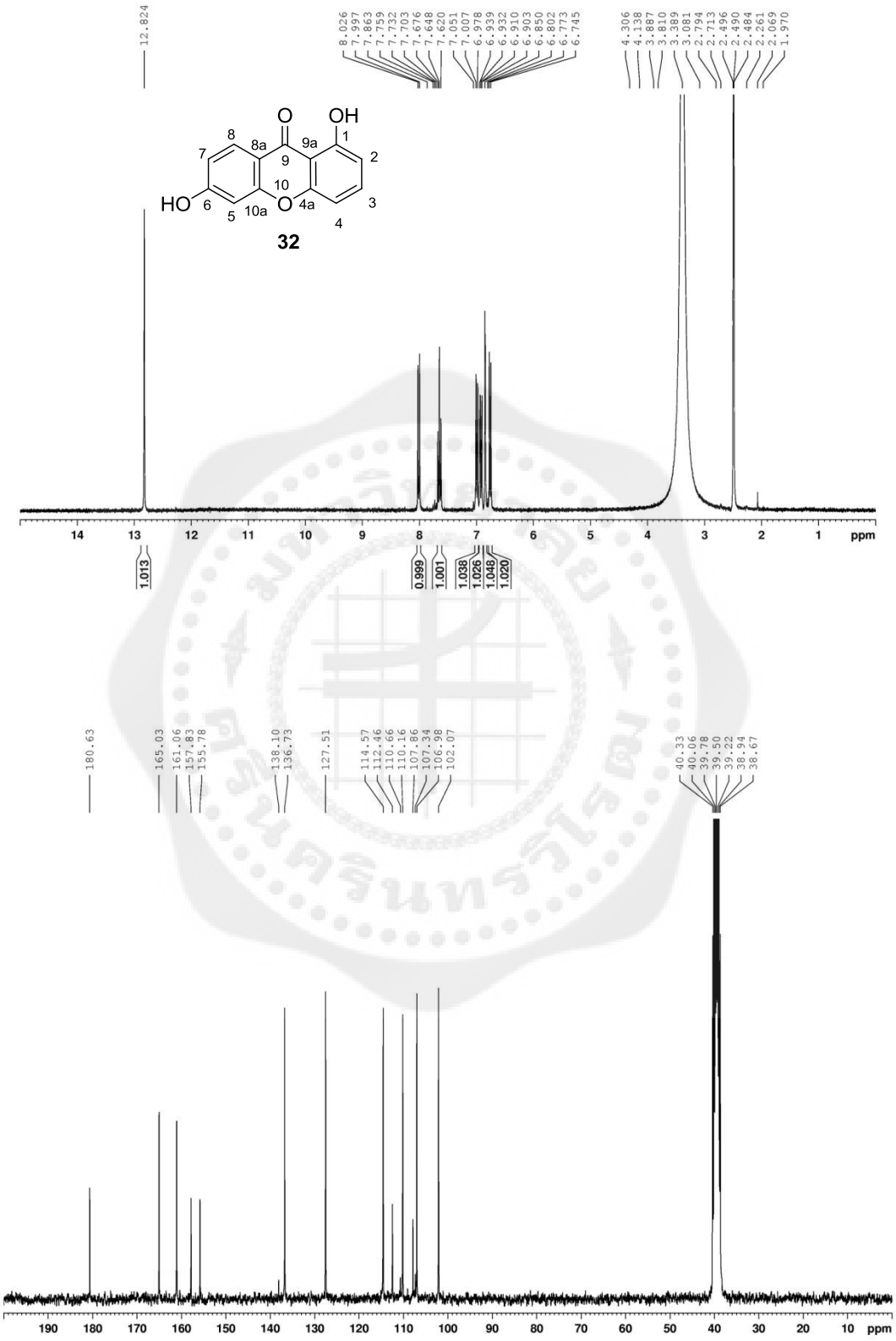


Figure 21 $^{1}$H- and $^{13}$C-NMR spectra of 1,6-dihydroxyxanthen-9-one (**32**) in DMSO-$d_6$

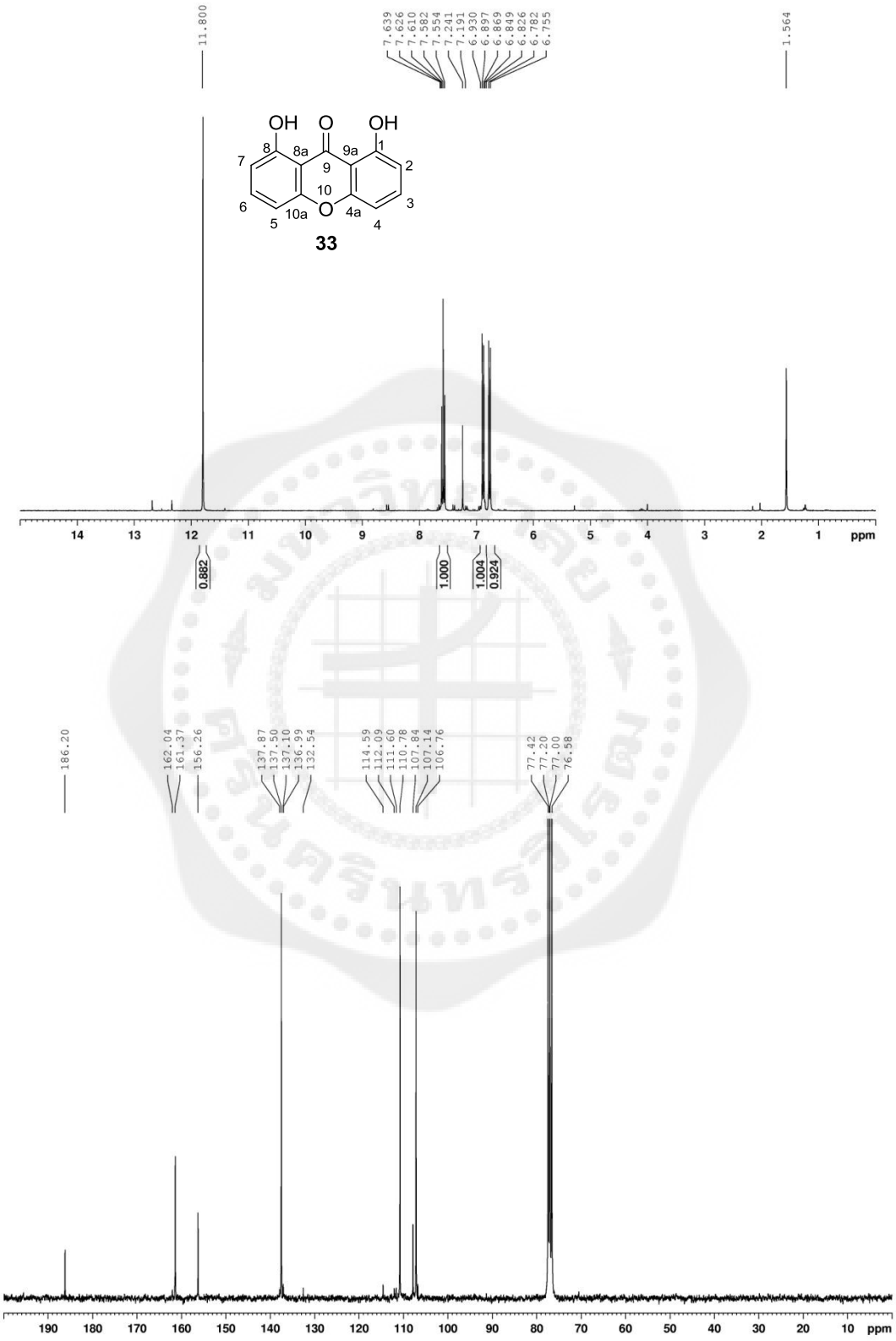


Figure 22 $^{1}$H- and $^{13}$C-NMR spectra of 1,8-dihydroxyxanthen-9-one (**33**) in DMSO-$d_6$

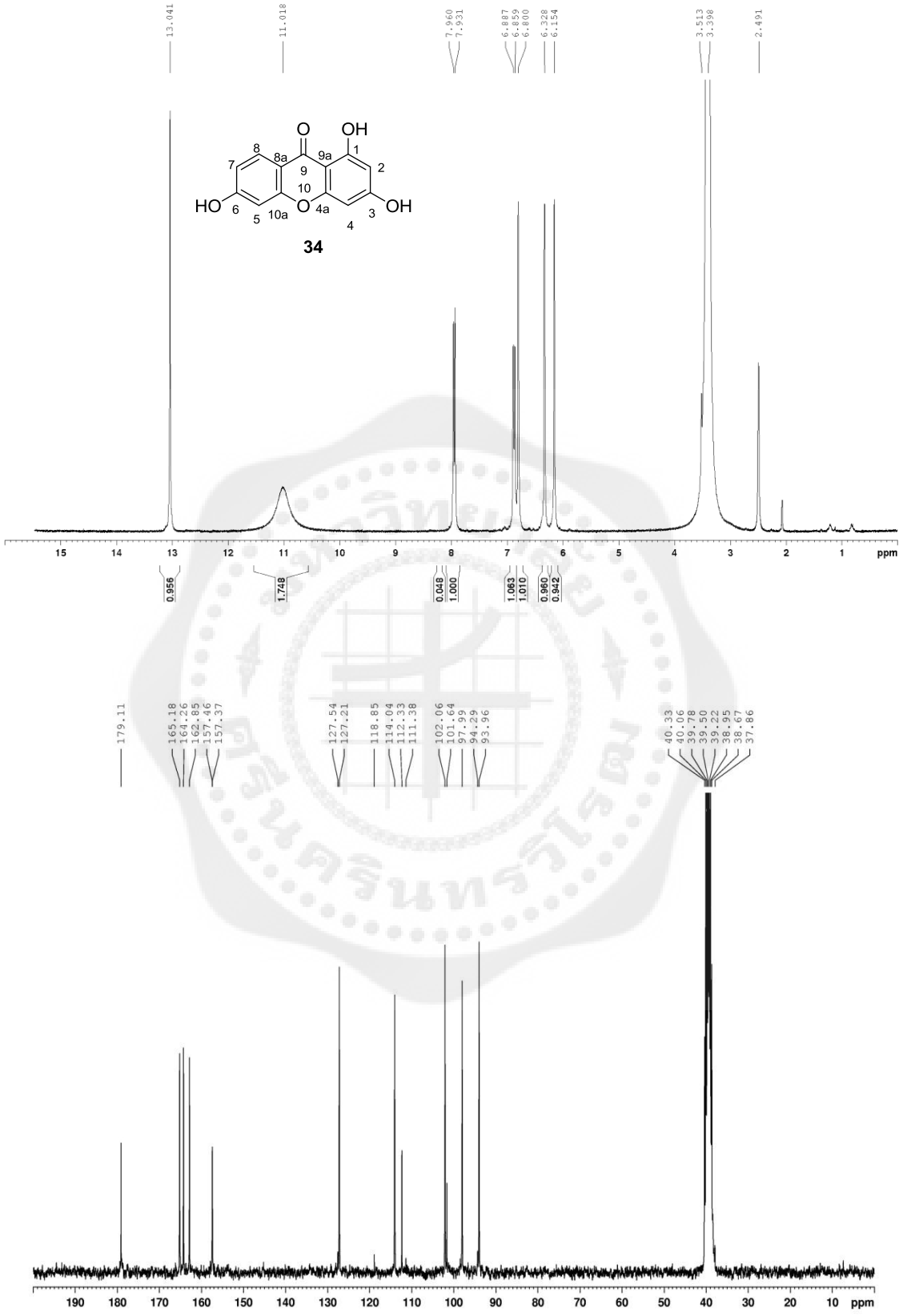


Figure 23 $^{1}$H- and $^{13}$C-NMR spectra of 1,3,6-trihydroxyxanthen-9-one (**34**) in DMSO-$d_6$

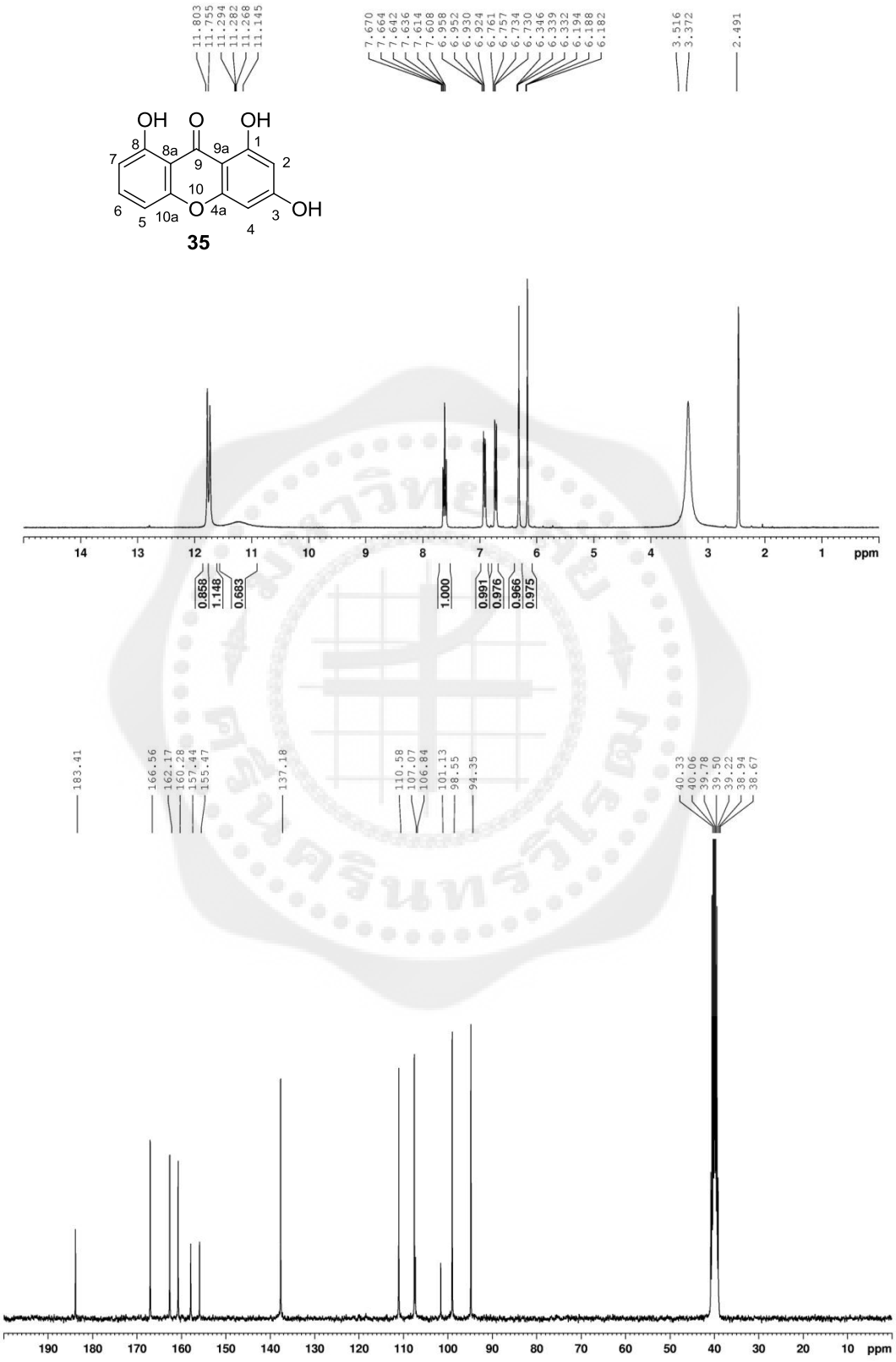


Figure 24 $^{1}$H- and $^{13}$C-NMR spectra of 1,3,8-trihydroxyxanthen-9-one (**35**) in DMSO-$d_6$

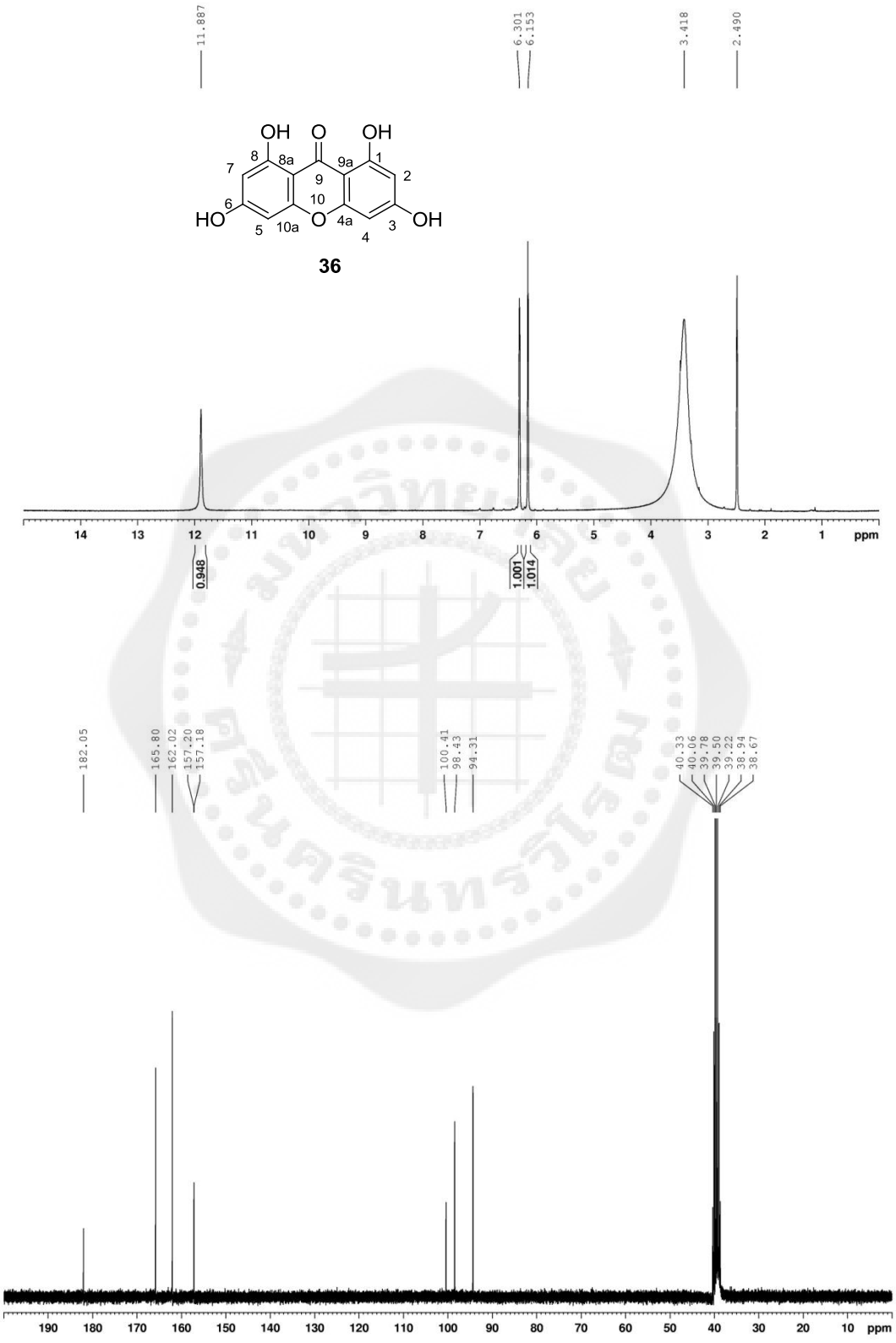


Figure 25 $^{1}$H- and $^{13}$C-NMR spectra of 1,3,6,8-tetrahydroxyxanthen-9-one (**36**) in DMSO-$d_6$

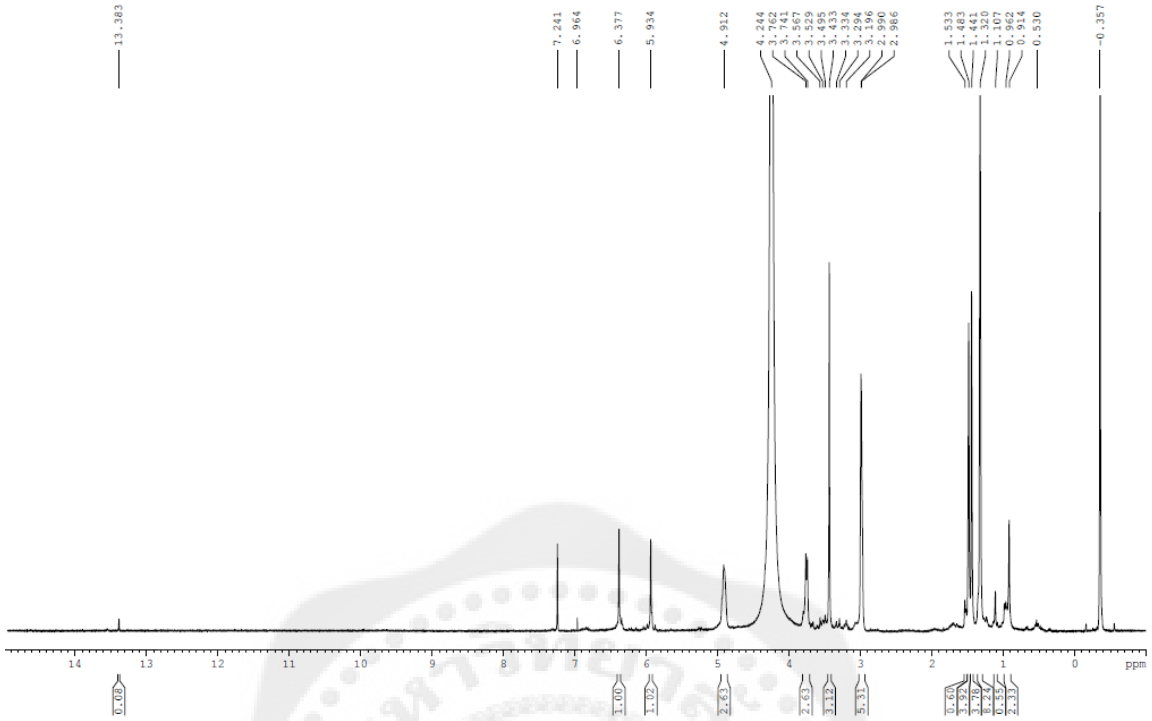

Figure 26 $^{1}$H-NMR spectrum of the $CH_2Cl_2$ fraction (**E5**) in $CDCl_3$ + $CD_3OD$

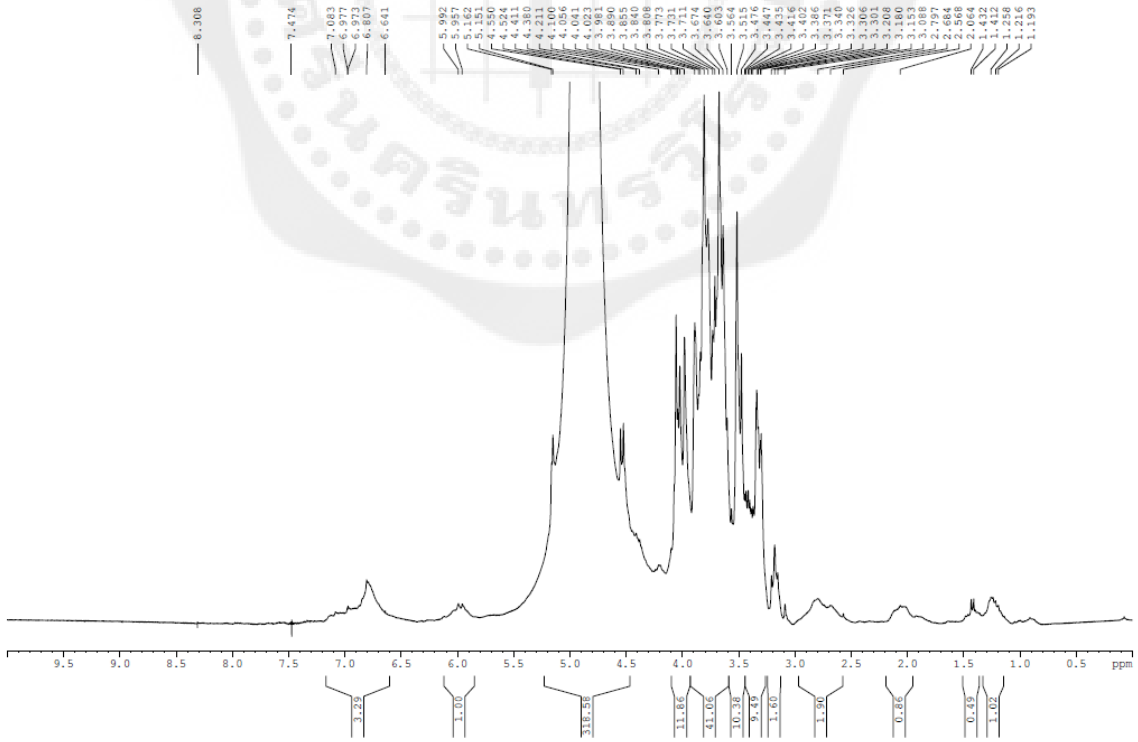

Figure 27 $^{1}$H-NMR spectrum of the aqueous fraction (**E6**) in $CD_3OD$

# GLOSSARY

# LIST OF ABBREVIATIONS AND SYMBOLS

| | | |
|---|---|---|
| ABC transporter | = | ATP-binding cassette transporter |
| ADP | = | Adenosine diphosphate |
| ATP | = | Adenosine triphosphate |
| CFTRact-09 | = | 8-Bromo-6-methyl-2,3,4,9-tetrahydro-1H-carbazol-1-one |
| $^{13}C$ NMR | = | Carbon-13 Nuclear Magnetic Resonance |
| Cacc | = | Calicium-activated chloride channels |
| NS004 | = | 1-(5-chloro-2-hydroxyphenyl)-5-(trifluoromethyl)-1H-benzo[d]imidazol-2(3H)-one |
| CC | = | Column chromatography |
| $IC_{50}$ | = | Concentration of drug required to inhibit enzyme activity by 50% |
| CFTR | = | Cystic fibrosis transmembrane conductance regulator |
| $\delta$ | = | Delta (Chemical shift for NMR data) |
| $CD_3OD$ | = | Deuteriomethanol |
| $CDCl_3$ | = | Deuteriochloroform |
| COSY | = | Correalation spectroscopy |
| DMSO-$d_6$ | = | Dimethylsulfoxide-$d_6$ |
| DPC | = | Diphenylamine-2-carboxylate |
| DEPT | = | Distortionless Enhancement by Polarization Transfer |
| d | = | Doublet (for NMR data) |
| dd | = | Doublet of doublets (for NMR data) |
| dt | = | Doublet of triplets (for NMR data) |
| ESI MS | = | Electrospray ionization mass spectra |
| DQC | = | Ethyl-2-(4-oxo-3-o-tolyl-3,4-dihydroquinazolin-2-ylthio)acetate |
| CFTRact-12 | = | 2-Ethyl-3-hydroxy-7,8,9,10-tetrahydro-6H-benzo[c]chromen-6-one |
| e.g. | = | For example |

# LIST OF ABBREVIATIONS AND SYMBOLS (continued)

| | | |
|---|---|---|
| G | = | genistein |
| g | = | Gram |
| $K_i$ | = | Haft-maximal inhibition |
| $IC_{50}$ | = | Half maximal Inhibitory Concentration |
| HMBC | = | $^1$H-detected heteronuclear multiple bond coherence |
| HMQC | = | $^1$H-detected heteronuclear multiple quantum coherence |
| MS | = | Mass spectrometry |
| m.p. | = | Melting point |
| m | = | Multiplet (for NMR data) |
| $\mu$g | = | Microgram |
| $\mu$L | = | Microliter |
| mg | = | Miligram |
| ml | = | Mililiter |
| GlyH-101 | = | *N*-2-(napthalenyl)-[(3,5-dibromo-2,4-dihydroxyphenyl)methylene]glycine hydrazine |
| nm | = | Nanometer |
| NMR | = | Nuclear magnetic resonance spectroscopy |
| NPPB | = | 5-Nitro-2-(3-phenylpropylamino)-benzoic acid |
| NOESY | = | Nuclear overhauser effect spec |
| KBr | = | Potassium bromide |
| $^1$H NMR | = | Proton nuclear magnetic resonance |
| UCCF-029 | | 2-Pyridin-7,6-benzoflavone |
| q | = | Quartet (for NMR data) |
| s | = | Singlet (for NMR data) |

## LIST OF ABBREVIATIONS AND SYMBOLS (continued)

| | | |
|---|---|---|
| PGA | = | Tannic acid |
| CFTRinh-172 | = | 2-Thioxo-4-thiazolidone |
| TLC | = | Thin layer chromatography |
| UV | = | Ultraviolet |
| V | = | Voltage |

CURRICULUM VITAE

# VITAE

**Name:** Watinee Kumpum

**Date of Brith:** November 16, 1988

**Place of Brith:** Bangkok

**Address:** 89/111 Moo 1 Lam Pla Thio Lat Krabanga Bangkok, Thailand 10520

**Education Background:**

2010 Bachelor of Science in Chemistry
Srinakharinwirot University, Bangkok, Thailand

2013 Master of Science in Chemistry
Srinakharinwirot University, Bangkok, Thailand

**Publcations:**

1. Luerang, W., Khammee, T., **Kumpum, W.**, Suksamrarn, S., Chatsudthipong, V., Muanprasat, C. (2012). Hydroxyxanthone as an inhibitor of cAMP-activated apical chloride channel in human intestinal epithelial cell. *Life Sciences* 90: 988-994.

**Poster presentation:**

1. Khammee, T., **Kumpum, W.**, Chatsudthipong, V., Muanprasat, C., and Suksamrarn, S. Hydroxyxanthone as CFTR inhibitor for treatment of cholera. PERCH-CIC Congress VIII. Jomtien Palm Beach Hotel & Resort Pattaya, Chonburi, Thailand, May 5-8, 2013. Poster number S2-P78.

2. Khammee, T., **Kumpum, W.**, Chatsudthipong, V., Muanprasat, C., and Suksamrarn, S. Hydroxyxanthone as CFTR inhibitor for treatment of cholera. CRMA Exhibition 2013. Chulachomklao Royal Military Academy, Nakhonnayok Thailand, November 20-21, 2013.